

A review on 3D micro-additive manufacturing technologies

Mohammad Vaezi · Hermann Seitz · Shoufeng Yang

Received: 27 June 2011 / Accepted: 30 October 2012 / Published online: 25 November 2012
© Springer-Verlag London 2012

Abstract New microproducts need the utilization of a diversity of materials and have complicated three-dimensional (3D) microstructures with high aspect ratios. To date, many micromanufacturing processes have been developed but specific class of such processes are applicable for fabrication of functional and true 3D microcomponents/assemblies. The aptitude to process a broad range of materials and the ability to fabricate functional and geometrically complicated 3D microstructures provides the additive manufacturing (AM) processes some profits over traditional methods, such as lithography-based or micromachining approaches investigated widely in the past. In this paper, 3D micro-AM processes have been classified into three main groups, including scalable micro-AM systems, 3D direct writing, and hybrid processes, and the key processes have been reviewed comprehensively. Principle and recent progress of each 3D micro-AM process has been described, and the advantages and disadvantages of each process have been presented.

Keywords Additive manufacturing (AM) · Direct writing (DW) · Microelectromechanical systems (MEMS) · Rapid micromanufacturing

1 Introduction

Nowadays, there is an enormous variety in microproducts, the major kinds being microelectromechanical systems (MEMS), micro-opto-electro-mechanical systems (MOEMS), and microelectronic products and micro-optical electronics systems (MOES) depending on the mixtures of product usefulness and operation fundamentals [197]. Due to the present tendency towards miniaturization of products in many industries comprising medical, automotive, optics, electronics, and biotechnology sectors [4], there is a demand for improvements in micro- and nanofabrication technologies and merging them in new manufacturing platforms.

A broad range of microfabrication technologies have been developed which have different applications and capabilities as their fundamentals are very diverse. Several classification schemes have been suggested by researchers to categorize microfabrication techniques. Masuzawa [171] focused on micromachining processes and classified them according to the implemented machining approach. Madou [167] categorized the microfabrication techniques as lithographic and non-lithographic methods. Perhaps the most widespread classification is that of Brinksmeier et al. [24] and Brousseau et al. [26] in which micromanufacturing has been classified in two generic technology groups: microsystem technologies (MST) and microengineering technologies (MET). MST encompass the processes for the manufacture of MEMS and MOEMS while MET cover the processes for the production of highly precise mechanical components, moulds, and micro-structured surfaces. An alternative classification was suggested by Dimov et al. [59] in which micromanufacturing technologies have been categorized according to their process “dimension” and material relevance.

Microfabrication technologies can also be categorized correspondingly as MEMS manufacturing and non-MEMS manufacturing [198]. MEMS manufacturing includes

M. Vaezi (✉) · S. Yang
Engineering Materials Group, Engineering Sciences,
Faculty of Engineering and the Environment,
University of Southampton,
Southampton SO17 1BJ, UK
e-mail: mv1y11@soton.ac.uk

H. Seitz
Fluid Technology and Microfluidics,
University of Rostock,
Rostock 18059, Germany

widely methods, such as laser ablation; plating; photolithography; lithography, electroplating, and molding (LIGA—German acronym); chemical etching; etc. Non-MEMS manufacturing generally includes methods, such as microextrusion, laser patterning/cutting/drilling, EDM, microinjection molding, microembossing, microstamping, micromechanical cutting, etc. [197]. Also depending on the used materials, microfabrication technologies are categorized as silicon-based and nonsilicon material microfabrication.

Many microfabrication processes have been developed up to the present, but such techniques are restricted when utilized to new microproducts which need the employment of a diversity of materials and have complicated three-dimensional (3D) microstructures with high aspect ratios. Recently, there has been fast improvement in micromanufacturing of 3D microstructures utilizing different methods and materials. Manufacturing technologies for 3D microcomponents play an important role in various areas of modern technologies in the evolution of very functional applications such as biochips, MEMS, microfluidic devices, photonic crystals, etc. [138, 144]. In MEMS technology, demand for fabricating complex microstructures from wide range of materials such as ceramics, metals, polymers, and semiconductor materials is observed.

MEMS technology will improve substantially if more complicated 3D microstructures can be created to fabricate integrated microsensors, medical devices, or micro-optical systems. Especially, fabrication of 3D microcomponents/assemblies which involve moving parts is a great challenge in micromechanics field. Some micromanufacturing methods such as soft lithography [259], laser photoablation [178], localized electrochemical deposition [166], the LIGA process [17, 69], etc., have been developed to promote the ability of the technology for more complicated microstructures. The LIGA process uses masked X-ray/laser radiation to incorporate thick resist layers to fabricate high aspect ratio microparts [11]. The LIGA process is restricted in producing 2.5D microparts and manufacture of complex 3D microstructure was still a challenge. Several processes have been examined for solving the critical problem of 3D micromanufacturing. In this way, the electrochemical fabrication (EFAB) process has been developed as an improved LIGA process to produce complicated 3D metal microparts layer by layer [47, 50]. Different 3D microparts can be produced using these methods from engineering materials, but majority of the processes (except EFAB) were developed for 2.5D micromanufacturing, which does not have the aptitude to produce a perfect and real 3D microparts. Multilayered photolithography [238] and deep proton writing [55, 240] were results of some earlier attempts toward true 3D microfabrication. New approaches such as micro-additive manufacturing (micro-AM) can also be considered to enhance capability of microfabrication technology in true 3D microcomponents manufacturing area.

2 Description and classification of 3D micro-AM

Among attainable alternatives, additive manufacturing (AM) processes that are based on layer-by-layer manufacturing are identified as an effective method to attain true 3D microproducts. 3D micro-AM can be classified into three main groups, including: scalable AM technologies which can be employed for both macro- and microscale, 3D direct writing (3DDW) technologies which have been merely developed for microscale and hybrid processes (Fig. 1).

AM technologies have been widely utilized within a decade with the purpose of producing complicated 3D components. Fabrication of 3D microparts/structures is also within the reach of some specific AM technologies via implementation of some essential modifications and improvements to get proper conditions for microfabrication. Scalable AM technologies, including: stereolithography (SL; which is called micro-SL (MSL) in microscale), selective laser sintering (SLS; which is called microlaser sintering (MLS) in microscale), 3D printing (3DP), inkjet printing processes, fused deposition modelling (FDM), and laminated object manufacturing (LOM) are the first group of the technology which have been regarded as a promising approach for true 3D micromanufacturing and can be employed efficiently to fabricate complex 3D microcomponents/assemblies. However, this class of micro-AM systems (except MSL) still suffers by some difficulties for microscale manufacturing as AM technologies have been developed mainly for normal-size fabrication. Some limitations of this group are due to its temperament and are same for both normal- and microsize manufacturing but some other limitations are for adaptation of this group for microsize manufacturing.

The second group of 3D micro-AM processes is 3DDW technologies. DW technologies have been developed basically for two-dimensional (2D) writing but some of DW methods such as laser chemical vapor deposition (LCVD), focused ion beam (FIB)DW, aerosol jet process, laser-induced forward transfer (LIFT), matrix-assisted pulsed-laser direct write (MAPLE), and nozzle dispensing processes (including precision pump and syringe-based deposition methods) can be utilized (or have potential) to produce high-resolution 3D microstructures/components. Among DW technologies, 3D-LCVD and FIBDW are used more efficiently to produce 3D microstructures. Nozzle dispensing techniques are currently used to produce 3D microperiodic structures for different applications. Aerosol jet process is served less for microfabrication of true 3D microstructures, but it has high potential for use in 3D applications. Some other DW approaches, such as LIFT and MAPLE can be used in a layer-by-layer process to build 3D structures, but they are still under development for micro-3D applications

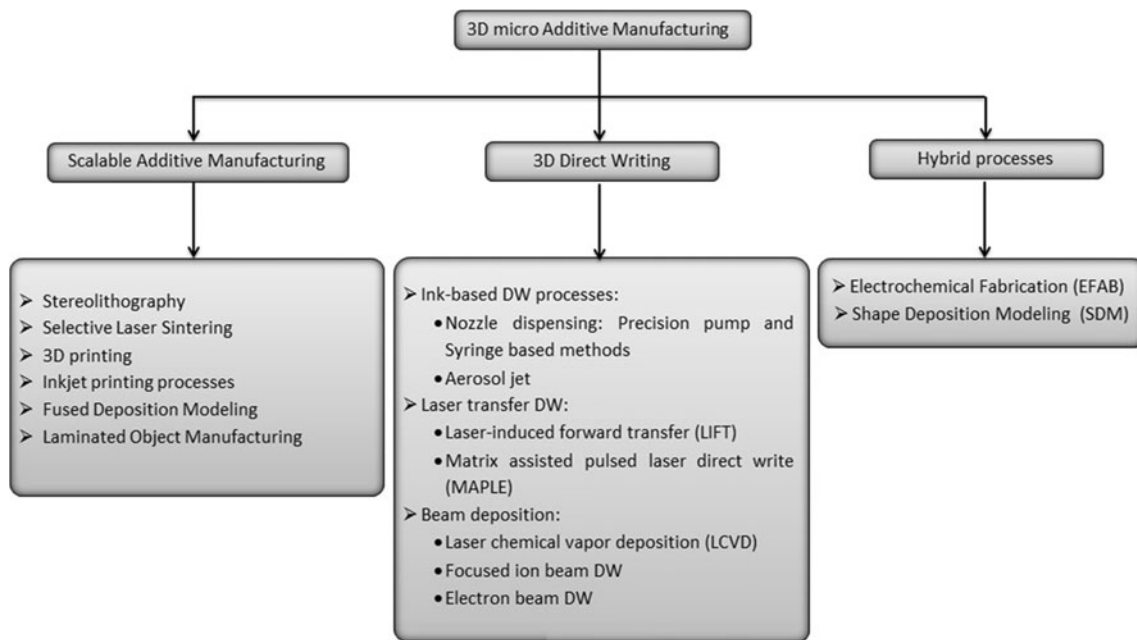


Fig. 1 Classification of 3D micro-AM processes

and a few research works have been reported on this issue. Overall, DW technologies need more improvements to become more compatible with 3D microfabrication, as most of DW methods have been developed normally for 2D purposes.

Hybrid processes including shape deposition modelling (SDM) and EFAB can be classified as the third group of the 3D micro-additive technologies. EFAB process uses electrochemical deposition and subtractive planarization in a layer-by-layer process to build 3D microstructures, while SDM process utilizes additive and subtractive processes sequentially to produce 3D microstructures. Among hybrid processes, the EFAB process has shown great applicability for true 3D micromanufacturing.

This paper presents a comprehensive review on the key micro-AM processes which are currently used effectively for true 3D microfabrication. Processes such as LIFT, MAPLE, aerosol jet, and SDM are not within the scope of this article since they are mostly employed for 2D/2.5D fabrication at the moment, although they have capability of 3D microfabrication. In the meantime, different nozzle dispensing DW techniques would be discussed along with FDM process (section 3.5) as they have same working principle (all are based on material extrusion), although they have been classified as direct writing techniques. It should be noted that the definitions from Madou [167] are accommodated in this paper for micromanufacturing. In this way, micromanufacturing applies to the manufacturing of components/products where the dimensions of at least one feature are in the micron scale.

3 Scalable AM processes

3.1 Stereolithography process

SL process is the first commercial AM process developed by 3D Systems Inc. and is based on layer-by-layer photosensitive resin polymerization using ultraviolet (UV) light. MSL is an additive 3D micromanufacturing process which was first introduced by Ikuta and Hirowatari [103] through developing the integrated hardened (IH) polymer SL and the improved super IH process [104]. MSL is on the basis of conventional SL, in which a light source radiates UV laser beam on a surface of a UV-curable liquid photopolymer, bringing about solidification of the photopolymer. MSL has submicron resolution for the x , y , z translational stages, laser spot has smaller diameter (a few micrometers) compared with classical SL, photopolymer solidification occurs in a very small area of the resin layer by layer and thus MSL enables to produce microparts with 1–10 μm -layer thickness. This micro-additive process is used in various areas such as micromachines and microsensors [218], microfluidic systems [105], optical waveguides [188], 3D photonic band gap structures [225], fluid chips for protein synthesis [275] and bio-analysis [19, 20]. Two main MSL techniques, namely, scanning MSL and projection MSL have been developed depending on the different beam delivery system.

The scanning MSL solidify the photopolymer (including UV photoinitiator, monomer, and other additives) in a point-by-point and line-by-line style in each layer. That was why Takagi and Nakajima [235] called this process as “vector-by-vector” MSL. Focal length of the laser should be very short to

reach laser spot sizes in a few micrometers. This results in troubles for scanning the laser beam. Thus, in optimized scanning MSL, the laser spot is focused by a dynamic lens and then the resin vat has been moved in x , y , and z directions for moving the laser spot instead of low-inertia galvanometric mirror (as is utilized in classical SL), which causes defocusing problem [103]. In this way, Xu et al. [261] developed a scanning MSL system with laser light spot with a diameter of $12.89\ \mu\text{m}$ on the focal plane and resin layers with a thickness of $20\ \mu\text{m}$.

In projection MSL, build time is saved significantly compared with the scanning MSL as whole layer of the photopolymer is cured once via exposure through provided mask. However, the first generation of projection MSL systems was slow and costly since a lot of projection masks had to be produced. In 1994, Suzumori et al. [234] proposed a SL system which utilized glass photo mask for exposure. The idea of mask-based MSL was ripened by Nakamoto and Yamaguchi [186]. In 2000, refrigerated MSL was utilized to create mask patterns via drawing an individual sol–gel transformable resin. To overcome the troubles included in the multiple mask process, the dynamic mask was used instead of multiple masks. The dynamic mask was used to electronically create pattern projection for exposure, with no need to replace the mask physically for each layer. In 1997, Bertsch et al. [19, 20] proposed that liquid crystal display (LCD) can be applied as the dynamic mask to control the expected pattern of each layer in the projection SL process. In LCD projectors, an array of light valves which is fabricated from liquid crystal material is applied as a projector to control the on/off of the UV light. Using LCD projectors caused reduction of the cost and solved the difficulties by the glass mask alignment. Monneret et al. [182] promoted the LCD-based MSL systems and Huang et al. [98] developed a LCD-based MSL system for direct mask photocuring. In 2000, a thin film transistor LCD was utilized by Hatashi [92] as a dynamic mask to produce optical lenses. Besides, the spatial light modulator as the dynamic mask and the UV light as the light source was used to intensify the microfeatures of the photomask image in area-forming rapid prototyping [37]. Some inherent defects of the LCD mask projection are: low switching speed ($\sim 20\ \text{ms}$), large pixel sizes, low filling ratio, low optical density of the refractive elements during the off mode, and the higher light absorption during the on mode [230]. Such defects (specially, large pixel size) restricted subsequent improvement of this technique for micromanufacturing.

Bertsch's research group [12] proposed that the digital micromirror device (DMD) which is embedded in Digital Light Processing projectors can be applied as the dynamic mask in MSL process. They used a metal halide lamp combined with optical filters to select a band of visible wavelength for the irradiation of the resin. In 2004, Stampfl et al. [222] used DMD-based MSL, in which visible

light is projected from below the resin vat to produce high-quality 3D microparts. Furthermore, UV light was utilized by Hadipoespito et al. [89] and Cheng et al. [39] instead of visible light, to cure the resin. The DMD is a semiconductor chip that has been developed by Texas Instruments® for high-quality digital projection. It involves many (around 1.5 million) micromirrors (each side at $\sim 13\ \mu\text{m}$) which are positioned in a matrix and each mounted on tiny hinges and can be individually controlled. Each micromirror stands for 1 pixel in the projected pattern and can be inclined autonomously at a small angle ($\pm 10\text{--}12^\circ$) via an electrostatic force to reflect the light and can repositioned quickly for turning the light on and off. As the resolution of the projected image is related to the size and number of the mirrors, high-resolution DMDs like $2,800 \times 2,100$ has been utilized in MSL to produce finer 3D microparts. To improve achievable resolution, DMD-based MSL systems are supplied with enhanced resolution module (ERM), whereby for each pixel built there are two exposures, shifted by half a pixel, which halves the native resolution of the system [28]. Figure 2 shows the difference between a standard DMD-based MSL and a DMD-based MSL supplied with ERM schematically.

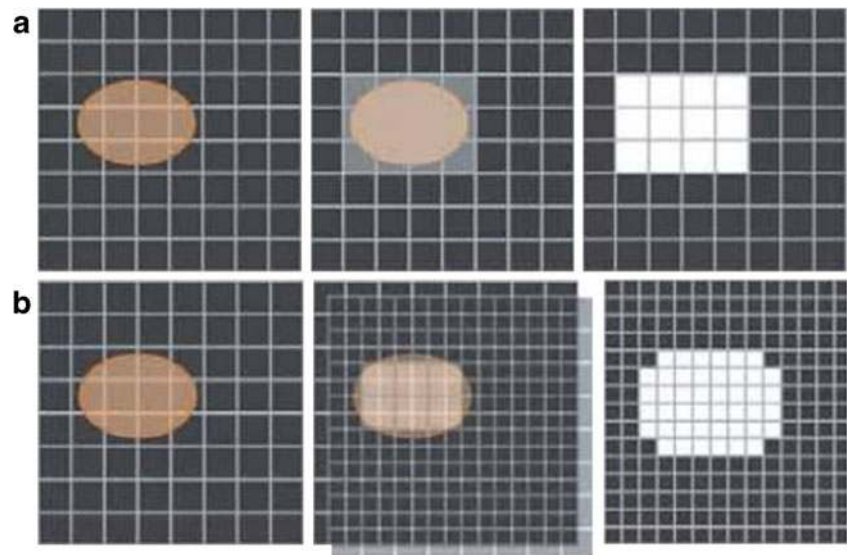
The Perfactory is a DMD-based micro-SL system supplied with ERM which has been commercialized by envisionTEC GmbH, Germany. The Perfactory system can build 3D microparts layer by layer (layer thickness down to $15\ \mu\text{m}$) with minimum pixel size of $30\ \mu\text{m}$ using ERM module. Figure 3 shows microparts with different blade thicknesses which have been fabricated in an experimental work by the authors with the use of the Perfactory micro-SL system. The minimum pixel size of $30\ \mu\text{m}$ can be observed in Fig. 3c.

Rapid microproduct development (RMPD) technologies is another projection MSL which have been invented and international patented by microTEC Gesellschaft für Mikrotechnologie mbH and the technologies are not based on US-patented DMD. It is possible to produce many microparts fast using microTEC technologies and also realize a higher resolution layer-by-layer (as thin as $1\ \mu\text{m}$) and surface quality in the sub-nanometer range using RMPD-nanoface technology [82].

RMPD writing system uses parallel laser beams, while RMPD mask uses UV light lamps and masks. In fact, RMPD mask is combination of mask technology used in photolithography and RMPD, which allows large-area exposure of the layers, and a considerable reduction of exposure time.

Several dynamic mask MSL systems have been developed by researchers up to now through the great ability of this micromanufacturing technology for fabricating complicated 3D microparts/components and batch fabrication of 3D Microsystems. Considerable attempts are also being made to employ a wide range of materials in MSL process for fabrication of MEMS with individual functions. In this way, different materials such as ceramics and metals as well as photocurable polymers have been utilized efficiently in MSL process [16,

Fig. 2 Scheme of pattern generation in DMD-based MSL systems; **a** standard and **b**) ERM modes [28]



40]. Especially, some biodegradable photocurable polymers have been utilized successfully in drug delivery systems and tissue engineering (TE) [132, 138, 144]. The process of research on development of MSL process has entered a new stage in a manner that efforts have been significantly increased toward optimization of process and its utility in new fields. Fabrication range is limited in MSL by the field of view of pattern generator (LCD or DMD) and the magnification of the objective lens. Ha et al. proposed a partitioned cross-section method for expanding the fabrication range while maintaining the fabrication resolution [88] and improving accuracy in the projection MSL system [190]. Zhou and Chen [278] developed a MSL system based on optimized mask video projection for improving accuracy and resolution. An experimental device was set up by Narahara et al. [187] to clarify the fundamental dynamic polymer solidification during polymerization. Based on the dynamic characteristic of photopolymerization, a dynamic finite element method was developed by Huang and Jiang [97] for simulation of photopolymerization process in MSL process with a single line radiation of laser. A theoretical model of solidification was proposed by Zissi et al. [280] and Scheffer et al. [208] in which concentration of the unreactive photoabsorber had been considered. In this way, effects of some

important parameters such as irradiation flux, photoinitiator concentration, and the irradiation time on the solidification depth were investigated and optimum width of single line laser radiation was proposed.

In MSL systems, minimum layer thickness is limited due to viscosity and surface tension of resin. Two-photon polymerization (2PP) process was developed by Maruo and Kawata [170]) to overcome this problem. They used a mode locked titanium (Ti)–sapphire laser emitting at 770 nm for the aims of manufacturing 3D microparts. In the 2PP process, the photoinitiator needs two photons to release a free radical that can initiate polymerization. In this way, the resolution of photopolymerization process increase considerably as only near the center of the laser is the irradiance high enough to provide the photon density necessary to ensure that two photons will strike the same photoinitiator molecule [82]. Kawata et al. developed a MSL apparatus based on the same principle with a 120-nm resolution using a femtosecond laser and built a microbull with 10 μm long and 7 μm high and about the size of a red blood cell [117]. Two scanning approaches are used in the 2PP process, including surface profile and raster scanings which do not need the resin to be layered in both methods. In surface

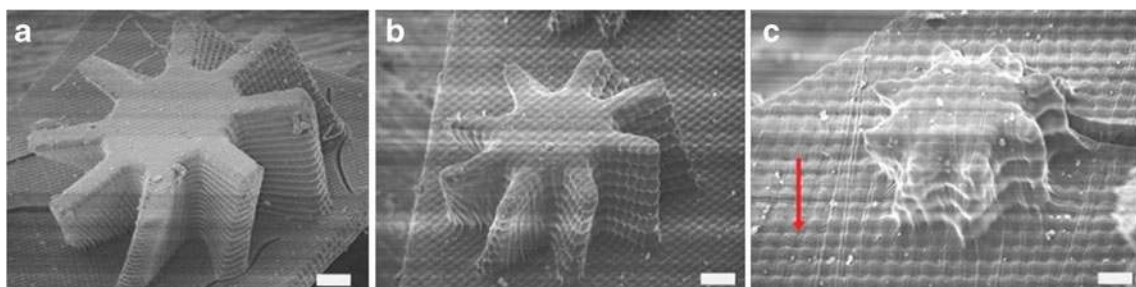


Fig. 3 Microparts fabricated by Perfactory MSL system—**a** blade thickness of 100 μm (scale bar, 120 μm), **b** blade thickness of 60 μm (scale bar, 100 μm), and **c** blade thickness of 30 μm (scale bar, 50 μm)

profile scanning, focusing of the laser beam and scanning in 3D inside the resin result in higher resolution compared with the layer-by-layer MSL process [277]. Figure 4 shows examples of microstructures produced by the 2PP process.

Different micro/nano-3D structures can be manufactured accurately using the 2PP process. By subtle focusing of a femtosecond laser beam in the 2PP process, it has been shown to be competent in obtaining a high spatial resolution of ~ 100 nm [191]. Several researchers have demonstrated the ability of the 2PP in 3D microfabrication for microrotors [79], micro-oscillators [117], optical memories [54], and photonic crystals [86, 219, 232]. Laser Zentrum Hannover used two-photon MSL with a femtosecond laser for manufacturing of a 3D microvenus [216]. Hill et al. [94] used Ti-sapphire lasers to fabricate 3D protein microstructures, containing cables and arches. Lim et al. [151] proposed an effective hybrid process (an additive process of two-photon caused polymer curing and a subtractive process of selective laser ablation) in which selective ablation-assisted 2PP was used to improve some of the limitations of the 2PP process. Also, new photoinitiators having enhanced two-photon sensitivity have been synthesized to increase quality of microparts [53, 273].

3.2 Selective laser sintering process

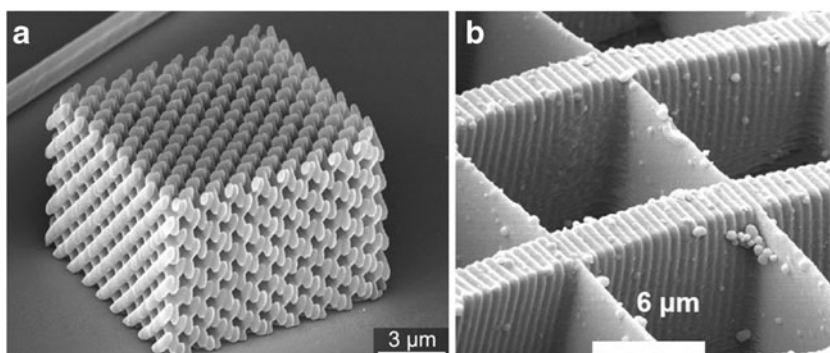
In SLS, a high-temperature laser is utilized to sinter layers of fine powders selectively. After each layer is produced, a roller spreads a fresh layer of powder on the bed and the process repeats until the part is completed [228]. Available commercial SLS systems are still unable to produce microcomponents that are smaller than $500\ \mu\text{m}$, as they have limited laser focus diameter ($50\text{--}300\ \mu\text{m}$). On the other hand, since SLS is a layer manufacturing process, thinner layers and correspondingly powders with smaller particle sizes are required to achieve finer details. As the finer particles have higher reactivity against humidity and oxygen, efficient approach must be applied to prevent powder corrosion. The process should be performed in a vacuum chamber to solve the hardships of humidity and oxidation. In addition, layers of finer powders are very loose due to prevailing interparticle forces [193].

Special collection approaches must be applied to prevent agglomerates. The extant shortage of layer density should be considered via a sufficient laser sintering procedure. Special powder deposition should be employed to overcome the mentioned issues. Haferkamp et al. [90] proposed a special roller-based powder deposition mechanism, including: rolls, powder reservoir, electric motors, a deposition carriage, and processing zone. The powder layer is formed and fed between two rolls working in opposite direction of rotation and is predeposited by a slide. The distance between the rolls is adjustable, whereby the thickness of the layer is variable (from 10 to $100\ \mu\text{m}$).

In 2003, The Laser Institute Mittelsachsen e.V. has proposed an innovative approach and a MLS system [66, 73, 201, 202], which was capable of producing microcomponents from ceramics and metals with an aspect ratio of up to 12, a resolution of less than $30\ \mu\text{m}$, and a minimum surface roughness of $1.5\ \mu\text{m}$. Specially, the process was a high potential approach for productive precision microtooling. The microcomponents produced by this process reveal a general maximum resolution of less than $30\ \mu\text{m}$, resolution of $20\ \mu\text{m}$ for ligaments, and resolution of $10\ \mu\text{m}$ for notches at aspect ratios of 12 and a minimal roughness R_a of $1.5\ \mu\text{m}$ can be obtained. With a 56-mm lens, $1,064\text{-nm}$ radiation can be focused onto a spot with a radius below $7\ \mu\text{m}$ [226]. The MLS can be connected to a turbo molecular vacuum pump to vacuum the build chamber down to a pressure of $10\text{--}3\ \text{Pa}$ and has a valve for utilization of different process gases during process [200]. A novel powder-coating system was applied to sweep the fine powder particle sizes over the build bed (as shown in Fig. 5a).

The powder feeding system included two special rakes that can be utilized for circular sweeping of powder materials onto the build bed. In this way, powder particle size and powder blend in each layer are easily controllable and there is a possibility for manufacturing multi- (Fig. 5a, b) or functional-graded material microcomponents. Also, there is a possibility to charge or flush process gases and so there is feasibility to combine laser sintering process with LCVD. More details of MLS system design can be found in Ref. [200]. Different microparts from various metals can be produced by MLS process. The process was launched into

Fig. 4 **a** 3D photonic crystal produced by 2PP process from photosensitive material. These structures can be replicated or inverted in silicon using silicon single-inversion and silicon double-inversion techniques (photo, Nanoscribe GmbH). **b** 3D microstructures in common photoresists (SU8) for investigating cell behavior on surfaces and in complex 3D containers (small walls are $300\ \text{nm}$) [211]



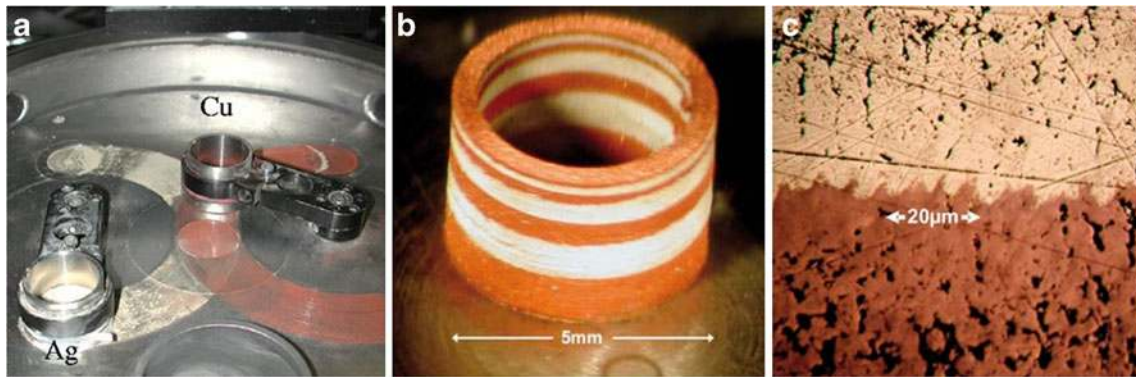


Fig. 5 Developed MLS system—**a** powder coating system with two rakes, **b** Multimaterial micropart from copper and silver, and **c** cross-section view of the interface between copper and silver sections, porosity can be realized [203]

the market by 3D-Micromac AG (Chemnitz, Germany) as “microSINTERING”. Figure 6 shows two 3D microparts produced by micro-SLS process, and Table 1 shows processed metal powders and particle sizes.

A critical challenge for MLS is the processing of nonmetallic materials. In the middle of 2005, first successful results were achieved in generating oxide ceramics bodies [71, 72]. But to fulfill the requirements of laser sintering of ceramics, it was necessary to develop new processing technologies and parameters [72]:

- The grain size of the powder has to be in the submicrometer range to reach a requested resolution of $40\ \mu\text{m}$ for this technique
- The absorption coefficient of the laser wavelength has to be high enough to transfer the laser energy into the material
- The generated sinter layers have to have a defined mean density of the material
- The processed material has to have a certain composition of glass and crystalline fraction to generate a satisfactory sinter quality

Selective laser melting (SLM) process is a rapid manufacturing (RM) technology which is very similar to SLS process. SLM employs higher energy density compared with SLS process, results in full melting of the powders and correspondingly achieving a much denser functional parts. Any specialized SLM system for micromanufacturing

has not yet been developed, and few works have been addressed to fabrication of microparts using SLM process [42]. However, the available commercial system SLM 50 of ReaLizer GmbH, Germany has the capability to produce fine features in the range of $40\ \mu\text{m}$, as it uses fine powders (smaller than $30\ \mu\text{m}$) and minimum layer thickness of $20\ \mu\text{m}$. A wide range of metals, including: super alloys, aluminum (Al), stainless steel, tool steel, cobalt (Co) chromium, and titanium have been processed successfully by ReaLizer’s SLM system.

3.3 Three-dimensional printing process

The 3DP process is based on inkjet technology and was developed at the Massachusetts Institute of Technology [41]. In this process, droplets of a binder material are deposited over the surface of a powder bed, sticking the powder particles together where the part is to be shaped. The process is followed by lowering the powder bed via a piston and a fresh layer of powder is spread over the previous layer and again binder is deposited over the surface of the new layer. This procedure is repeated to build whole of the part [207]. 3DP has demonstrated the capability of fabricating parts of a variety of materials, including ceramics, metals, shape-memory alloys (SMA) and polymers with an array of unique geometries [34, 157, 215,

Fig. 6 3D microparts produced by MLS process [203]

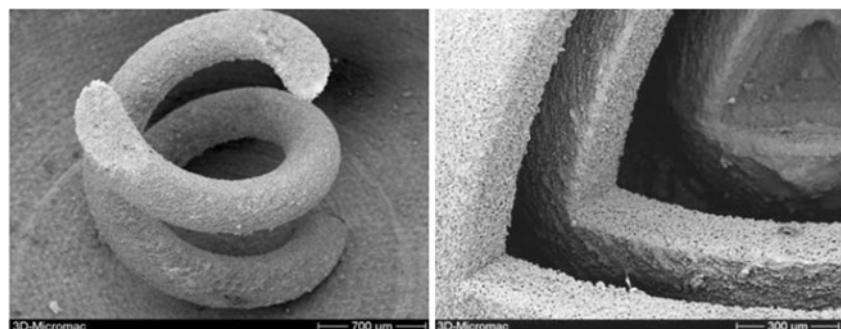


Table 1 Processed metal powders and their grain sizes [73]

Materials	Copper	Tungsten	Silver	Aluminum
Particle size	10 μm	300 nm	2 μm	3 μm

250]. 3DP allows the design and fabrication of complicated scaffold shapes with a fully interconnected pore network with both a novel micro- and macroarchitecture [131].

In 3DP process, larger particles have lower surface per volume and are simpler for spreading [156] and have larger pores results in fabrication of more homogeneous parts as binders can immigrate better inward the powder bed [23]. But like microsintering process, thinner layers and correspondingly powders with smaller sizes are required to achieve finer details (microscale features). Finer powders have the potential profits of lower surface roughness, thinner layers, and promoted printability [206]. Also micro-3DP technology utilizes high-resolution piezoelectric printing heads instead of thermal printing heads (as used in normal-size 3DP) for building 3D microparts.

Digital Metal™ is a precision inkjet technology developed by Fcubic AB, Sweden for 3DP of micrometal components with a resolution of 20 μm and a surface finish of approximately 4 μm (Ra). Digital metal technology offers unique capacity to rapidly produce highly complex and intricate designs and features for micron size metallic parts, cost-effectively in low-to-medium volumes. This process utilizes 3DP and sintering process as a post-processing to produce high-accuracy microcomponents. In this process, a special sintering aid is spread as a binder over the powder in the areas which are part cross-section, in this way the area will fuse more quickly in a sintering furnace. By applying sintering aid as a binder, the part will sinter in at lower times and temperatures in the furnace than encompassing powder that has not gotten sintering aid. An important benefit of the micro-3DP process is that it is significantly a faster process compared with other micro-additive processes and so it can be utilized for direct mass production of microparts as well as microprototyping [111, 113]. In a collaborative work with Fcubic AB, the authors have evaluated the capability of Digital Metal 3DP process for 3D thread fabrication. The result has been presented in Fig. 7. In this experimental work, the resolution of the process for the part was 20 μm in x and y and 40 in z directions.

Also, 3DP process can be applied efficiently for direct fabrication of microceramic molds. Charmeux et al. [36] investigated the manufacturability of microzirconia ceramic shells via 3DP for less expensive and a faster investment casting of microcomponents. Dimov et al. compared the capabilities of the micro-3DP process to common two-stage investment casting to build metal microparts. This comparative research work is concerned with the fabrication of sample microcomponents from stainless steel and Al/zinc

alloys with features in the range of 250 to 700 μm and aspect ratios up to 2.4. Corresponding to their report, micro-parts from Al and zinc alloys with features in 250 and 500 μm and aspect ratio of 2.4 could be produce by 3D printed ceramic micromolds with accuracy around 5 and 20 % of the nominal dimension, respectively.

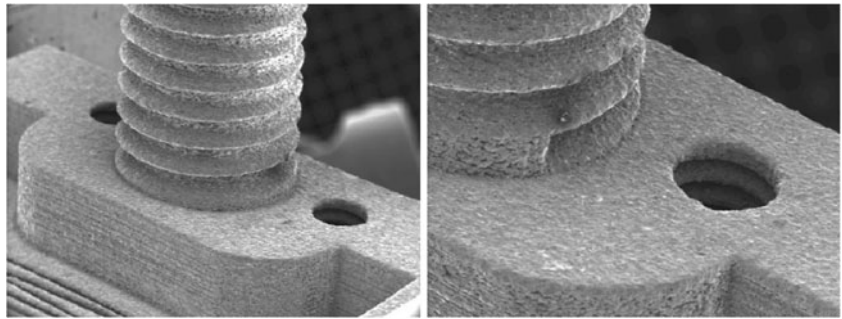
3.4 Inkjet printing processes

Inkjet printing processes are based on inkjet technology and include arrangement and layer-by-layer deposition of a liquid material in droplet form. Droplets of liquid materials usually called fluid or ink. The material often turns into solid subsequent to the deposition process via cooling (e.g., by crystallization or vitrification), chemical changes (e.g., through the cross-linking of a polymer), or solvent evaporation. Also, other post-processing procedures like sintering could be included.

In inkjet printing technology, two different techniques prevalently are utilized for droplet creation, namely, drop-on-demand (DOD) and continuous inkjet (CIJ). Generally, CIJ systems operate with fluids of lower viscosity than DOD and at a higher drop velocity [96] and so DOD technique has more potential for 3D microfabrication. In DOD technique, ink droplets are solely delivered when they are demanded to be printed. Thus, there is no necessity for unused liquid recycling. The droplets of desirable material are ejected from an ink vat in reaction to an activate signal, through pressure pulse which is generated by an actuator. There are two main kinds of actuator: thermal and piezoelectric actuators. In thermal DOD, a transitory bubble of vapor is created by fast and glancing heating of the ink using a small electrical heating element situated in the ink reservoir close to the print head nozzle. Creation of this bubble of vapor results in injection of a jet of ink from the nozzle. The thermal DOD technique (also called bubble jet) is broadly utilized in typical office printers. The piezoelectric element is the more common industrial system which makes a change in the internal volume of the ink reservoir using an electric field to create pressure waves. The pressure waves results in ink ejection from the print head nozzle and afterward correspondingly filling again the reservoir [96]. Vaporization of small volume of the ink results in consequential limitations on the usable materials in the thermal DOD process. The materials must be comparatively volatile (or have a component which is volatile), while, the piezoelectric DOD method has no such limitation. For both mentioned methods of DOD, print heads usually include several separate nozzles which are fed via a single-ink manifold in a participatory manner but each separately controllable.

Turning of the fine droplets into solid (phase transition) can also be accomplished by curing of a photopolymer ink using UV light in inkjet printing process. Two inkjet printing systems, including: Eden printer by Objet Geometries and ProJet printer by 3D Systems have been commercialized based on

Fig. 7 3D microthreads fabricated in a collaborative research work using Fcubic process, outside M5 thread and two M2 inside threads



the same principle. Objet's printers use special print heads with many individual nozzles to deposit a number of different acrylic-based photopolymer materials with 42- μm resolution and in 16- μm layers. Each photopolymer layer is cured by UV light immediately as it is printed, producing fully cured models. Support structures are built in a gel-like material, which is removed by hand and water jetting [82]. ProJet printer uses the same technique barring that support structure used with this machine is a wax which has a much lower melting temperature than the part printed and is easily melted out. This method of "hands-free" support removal allows for highly complex 3D micromounts/assemblies and delicate applications. Figure 8 shows sample microparts with 400- μm blade thicknesses which have been fabricated via different commercially available inkjet-based systems, including Eden 260 V, ProJet HD 3000plus, as well as Solidscape's T76 3D printer which is a commercial piezoelectric DOD micro-AM system for printing of polymer inks.

As seen in Fig. 8, the blade produced via ProJet 3000 HD has better dimensional stability and surface quality than Eden 3D printer due to higher resolution (34 μm) and hands-free support removal. Support material between some blades can be seen in ProJet's micropart, although it has a smoother surface than Eden printer. Better finishing may solve this problem. The edges of the blades are sharper in Solidscape's micropart, and they have better surface quality as compared with ProJet and Eden printers. Nevertheless, some extra material (not support material) can still be seen between blades in Solidscape's

micropart. It is believed that the most important limitation of inkjet printing systems is currently support removal for complex 3D microstructures. In the meantime, resolution of the process should be improved to expand the range of applications.

Other specialized piezoelectric DOD microfabrication systems have been developed by MicroFab technologies, USA for high-quality micropart fabrication. MicroFab's DOD technology has been used by many researchers to investigate effective parameters on microdroplet generation. Figure 9 shows typical experimental set up used by Ko et al. [124] in which build plate can move in x and y directions and metal nanoparticles (NP) droplets are observed by a CCD camera.

In such DOD experimental system, droplets are ejected through voltage waveform changes (Fig. 9 inset graph). In short, the first rising voltage expands the glass capillary and a droplet is pushed outside the nozzle due to the falling voltage. The final rising voltage cancels some of the residual acoustic oscillations that remain after drop ejection and may cause satellite droplets. The signal generator used to produce microdroplets also triggers the CCD camera, so that the CCD captures images at the droplet generation frequency [124].

Viscosity, inertia, and surface tension are three main factors which affect the behavior of drops and liquid jets. Some dimensionless parameters such as Reynolds number (Re), Weber number (We), and Ohnesorge number (Oh) are used for describing and analyzing jetting and break-up phenomena in microdroplet generation. The Re is a

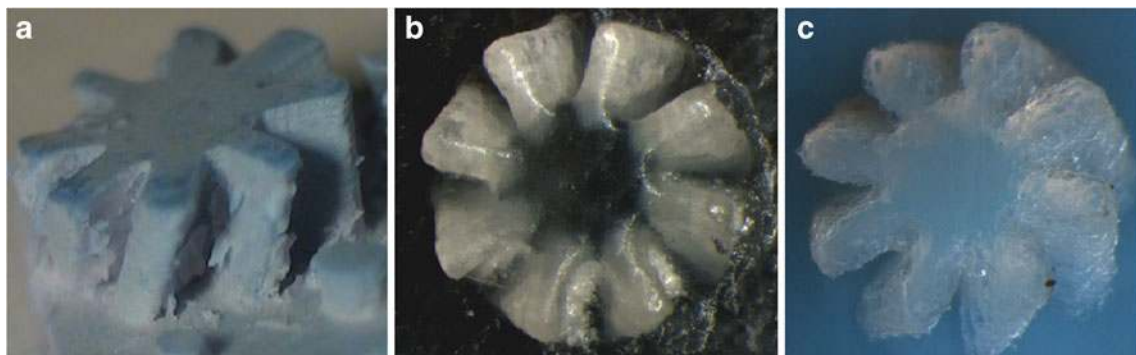
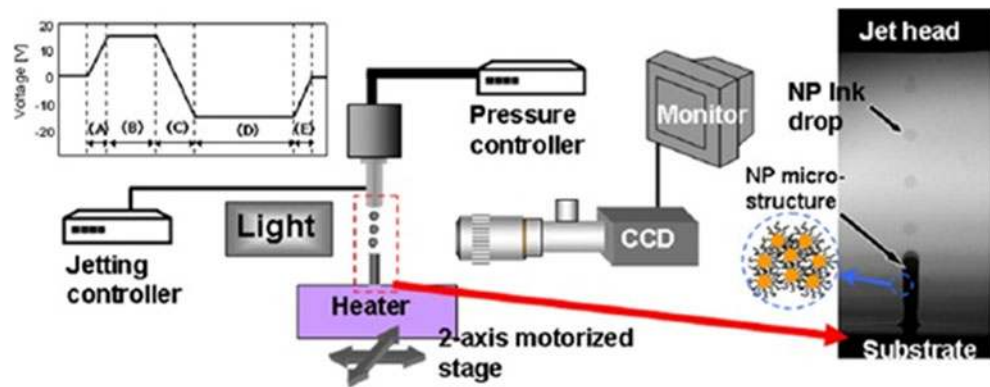


Fig. 8 Sample microparts with 400 μm blade thickness produced using different inkjet printing systems—**a** Solidscape's T76, the part was made with $\sim 5\text{-}\mu\text{m}$ resolution and in 12.7- μm layers; **b** 3D System's ProJet HD

3000plus, the part was made in the extreme high-definition modus (34- μm resolution and 16- μm layers); and **c** Objet's Eden 260 V 3D printer, the part was made with (42- μm resolution and in 16- μm layers)

Fig. 9 Typical piezoelectric DOD printing system [124]



characteristic which describes the ratio between inertial and viscous forces and obtained by $Re = \rho dv / \eta$, where v is fluid velocity, η is dynamic viscosity, d is specific length (droplet diameter), and ρ is fluid density. The We is a characteristic which describes the ratio between kinetic energy and surface energy: i.e., between inertial and surface forces and obtained by $We = \rho dv^2 / \delta$, where δ is surface tension. Also, the Oh is a characteristic which describes the relative importance of viscous and surface forces and obtained by $Oh = We^{1/2} / Re = \eta / (\rho \delta d)^{1/2}$ [96]. According to research works of Wang et al. [255] and Derby and Reis [56], for $Oh > 1$, fluid viscous dissipation results in orifice clogging and impedes ejection of drops and also for $Oh < 0.1$ multiple drops is produce instead of a single well-defined drop. So, in practice, jettability criterion for precision DOD printing is $1 > Oh > 0.1$ and correspondingly droplet velocity should be 5–10 m/s. Table 2 shows jettability criterion for both CIJ and DOD processes. It should be noted that for non-Newtonian fluids, other parameters such as the Weissenberg number (Wi) is used to blend the effects of viscoelasticity. The Wi value can be obtained by $Wi = Tv / d$, where T is a characteristic relaxation time of droplet [96, 150].

Disturbance frequency has important effect on formations of jet and break-up [148]. The optimum disturbance frequency (f_{opt}) can be estimated in the following equations [109]:

$$f_{opt} = \frac{v_j}{\pi d_j \sqrt{2(1 + 3ZO_h)}} \quad (1)$$

$$v_j = k \times v_0 \quad (2)$$

$$v_0 = \frac{2}{3} \sqrt{\frac{3\Delta P}{\rho_j} + \frac{1,024\mu_j^2}{d_0^2\rho_j^2}} - \frac{64\mu_j}{3d_0\rho_j} \quad (3)$$

Where d_j is jet diameter, ΔP is gas pressure in the ink reservoir, d_0 is orifice diameter, ρ_j is ink density, μ_j is jet viscosity and is jet velocity which has direct relation with orifice velocity v_0 . The orifice velocity as well as the jet velocity increases with the gas pressure in the ink reservoir.

Coefficient k should be calibrated for the different nozzles and the materials [109]. The influences of the disturbance frequency on the droplet generation for two different fluids, namely, water and Sn63/Pb37 metallic ink were investigated by Jiang et al. [109]. As an example, Fig. 10 shows the images of water droplet generation which were captured by the high-speed CCD camera.

As seen in Fig. 10b, c, e, the droplets merge with each other to form bigger droplets due to the difference of the droplet velocities. According to this visual experiment, the satellite droplets and the merged droplets cause degradation of the droplet diameter accuracy. As seen in Fig. 10d, when the imposed disturbance frequency is selected properly, the droplets are round with uniform sized and spaced with the same distance [109].

Inkjet printing is used for microprinting of both metallic and nonmetallic (usually polymers) materials but DOD printing of metal inks needs special configurations to control jetting process for achieving well-defined droplets. For example, jetting process should be performed in a low-oxygen environment to avoid the oxidation of the jet and the microdroplets. Researches have demonstrated that the molten metal in high oxygen environment reacts with oxygen to form a surface oxide layer which changes the physical properties of the jet surface and prevents the jet from disintegrating [130,

Table 2 Comparison of droplet parameters for standard commercial continuous inkjet (CIJ) and drop-on-demand (DOD) printers (taken from [96])

Parameters	DOD	CIJ
Fluid viscosity (mPas)	10–100	2–10
Droplet diameter (μm)	10–150	10–150
Droplet volume (pL)	0.5–2,000	0.5–2,000
Droplet velocity (m/s)	5–10	10–20
Reynolds No.	2–50	100–1,000
Weber No.	50–150	500–1,500
Ohnesorge No.	0.1–1	0.03–0.2

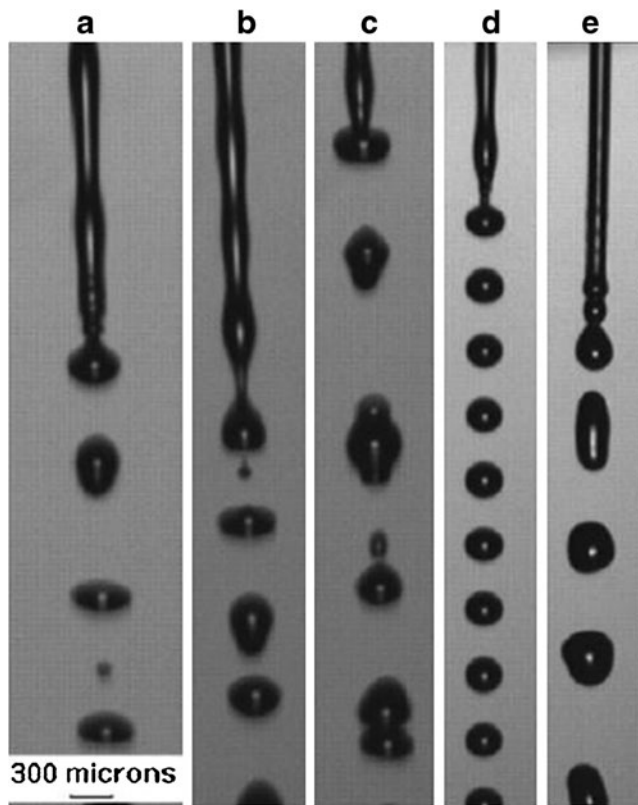


Fig. 10 Captured images of water microdroplet generation using orifice diameter of 150 μm at a gas pressure of 8 kPa—**a** $f=0$, **b** 1,000, **c** 2,000, **d** 2,842, and **e** 3,500 Hz [109]

271] and uniform-sized alloy droplet stream is produced in the argon environment where oxygen concentration is no more than 10 ppm [148].

Overall, successful inkjet printing of 3D microstructures of metal inks could be achieved within a certain jetting condition range. The basic requirement conditions for successful metal ink DOD are (1) stable jetting droplet generation, (2) sufficient droplet drying before the subsequent droplet arrives, and (3) a stable base structure initiating the 3DP. The three requirements are strong functions of ink properties (viscosity and surface tension), jetting parameters (signal width, voltage magnitude, and frequency), and environment (pressure, temperature, and humidity). Those parameters are strongly interconnected. However, the most fundamental inkjet printing parameters are (1) jetting frequency (as discussed above) and (2) substrate temperature [124]. An interesting research work was performed by Ko et al. [124] to investigate the effect of substrate temperature on the NP inkjet printing. They examined five regimes to obtain the optimum inkjet printing condition. According to their work, proper substrate temperature allowing sufficient drying of the NP inks in each layer is essential for a successful 3DP.

3.5 Fused deposition modeling and extrusion-based techniques

Extrusion-based AM systems utilize a computer-controlled deposition nozzle to create patterns and 3D objects with controlled composition and architecture. These processes have same working principle so as they deposit material in form of continuous flow, and they can be basically classified into two main groups: processes based on material melting and processes without material melting. FDM process and its variations, such as precision extrusion deposition (PED) [255], 3D fiber deposition [258], precise extrusion manufacturing (PEM) [260], and multiphase jet solidification (MJS) [84] are AM techniques with material melting. Pressure-assisted microsyringe (PAM) [252], low-temperature deposition manufacturing [279], 3D bioplotting [134], robocasting [35], direct-write assembly [221], and solvent-based extrusion free-forming [85] are the most commonly used AM techniques without material melting. Four major nozzle designs have been exploited in nonheating processes: pressure-actuated, volume-driven injection nozzles (normally using a stepper motor), solenoid and piezoelectric actuated, whereas two main nozzle designs including filament driving wheels and mini-screw extruder have been used in processes with material melting.

There are very few reports on utilization of extrusion-based systems for fabrication of true complex 3D microparts. In particular, there are some essential limitations for applying extrusion-based systems with material melting in microfabrication area. The volume of flow should be in the order of nanoliters per second and rod width should be reduced up to 20–30 μm (and correspondingly layer thickness) for microfabrication and this needs an accurate molten flow delivery and control systems. In the meantime, there is demand for precise temperature control system to achieve desirable accuracy.

However, there has been great trend on applying extrusion-based systems in fabrication of 3D microperiodic structures such as tissue engineering (TE) scaffolds with micro-sized rod/pore. FDM has been used to successfully produce TE scaffolds in poly(ϵ -caprolactone)PCL, polypropylene/tricalcium phosphate (PP/TCP), polycaprolactone/hydroxylapatite (PCL/HA), PCL/TCP, PP/TCP, and poly(lactide-coglycolide) (PLGA) with resolution of 250 μm [99, 114, 274]. Bone TE scaffolds produced from polymer and CaP using FDM process have exhibited good mechanical and degradation properties, improved cell seeding, and enhanced incorporation and immobilization of growth factors. As for mechanical properties, existence of CaP phase brings about higher structural strength and polymer phase provides plasticity and toughness to the scaffold.

Modified FDM systems such as PED, 3D fiber deposition, PEM, and MJS have been developed to overcome

FDM limitations in terms of feedstock shape and resolution. New configurations for melt extrusion could open up the possibility for the use of a wider range of biomaterials, making the extrusion-based systems more versatile and realizable alternative manufacturing process for composite scaffold materials. Nevertheless, there was still limitation in terms of the high heat effect on raw biomaterial and resolution of the process. Thus, researchers made attempts to develop new configurations without material melting that can better preserve bioactivities of scaffold materials. PAM process is a technique developed by Vozzi et al. [252] that resembles FDM process without the need for heating. PAM uses a pneumatic driven microsyringe to deposit biomaterial on a substrate with resolution of 10 μm . Polymeric scaffolds with different polymers compositions such as PCL, poly(L-lactic acid) (PLLA), PLGA, PCL/PLLA, gelatin, and alginate hydrogels scaffolds with three different geometries-square grids, hexagonal grids, and octagonal grids were produced [168, 241, 242, 251, 253]. Vozzi's group used a modified system called piston-assisted microsyringe for microfabrication of viscous, sol-gel, or gelled inks (e.g., alginate solutions at different concentrations) [243].

3D bioplotting is a technique that was first developed by Landers and Mulhaupt [134] at Freiburger group to produce 3D scaffolds with micron sized rods for soft tissue engineering purposes, and simplifying hydrogel manufacturing. In this process, the material dispensing head normally moves in three dimensions, while the fabrication platform is stationary. Either a filtered air pressure (pneumatic nozzle) or a stepper motor (volume-driven injection nozzle) is used to plot a viscous material into a liquid (aqueous) plotting medium with a matching density. It is possible to perform either a discontinuous dispensing of micro dots or a continuous dispensing of fine filaments. In comparison to other extrusion-based SFF processes, 3D Bioplotting can process a remarkably wide variety of different biomaterials, including polymer melts, thermoset resins, polymer solutions, and pastes with high filler contents, bioactive polymers such as proteins. The plotting of biomaterials such as melts of PLA, PLGA, poly-(hydroxybutyrate-co-valeriate) biodegradable thermoplastic, PCL, and poly(butylene terephthalate-block-oligoethylene oxide), biopolymer solutions of agar and gelatin [133], natural polymers, such as collagen, and reactive biosystems involving fibrin formation and polyelectrolyte complexation is possible. 3D bioplotting can process thermally sensitive biocomponents, and cells since heating is not applied.

Khalil et al. [118] developed a special multinozzle bioplotter which was capable of extruding biopolymer solutions and living cells for freeform construction of 3D tissue scaffolds. The deposition is not occurred into plotting media but is biocompatible and occurs at room temperature and low pressures to reduce damage to cells. Ang et al. [5] set up

a special robotic bioplotting device called rapid prototyping robot dispensing (RPBOD) for the design and fabrication of chitosan-HA scaffolds. Furthermore, the RPBOD system was improved to include a new manufacture method, called dual dispensing system as besides the pneumatic dispenser, a mechanical dispenser which was driven by a stepper motor was set up to deposit plotting medium [133].

Variety of extrusion-based AM techniques has also been developed for processing of ceramics. Robocasting is a technique in which a computer controls the deposition of highly concentrated (typically 50–65 vol% ceramic powder) colloidal ceramic slurries. Solvent-based extrusion free-forming is a ceramic processing technique developed by our research group to produce bioceramic scaffolds [266–268, 270] and electromagnetic band gap materials [11]. In this process, continuous flow of materials in form of paste or particulate slurries is dispensed on to the surface using a 3D motion system incorporated with the nozzle. Solvent-based extrusion freeforming is relatively simple process in which phase change is based on solvent evaporation. Paste with high yield strength is prepared by blending polymer, ceramic, and a solvent with specific ratios. Defects such as dilatancy, drying cracks and surface fracture which happens in water-based extrusion systems can be eliminated by appropriate adjustment of polymer content [269].

Direct-write assembly is an extrusion-based system developed by Lewis et al. [221] whereby a wide range of inks can be patterned in both planar and 3D shapes with feature sizes as fine as 250 nm. In this process, compressed air is employed to push inks with controlled rheological properties through an individual nozzle (diameter ranging from 1 to 500 μm). Direct-write assembly deposits inks at room temperature or a proper coagulation reservoir using a controlled-printing speed and pressure which depend on ink rheology and nozzle diameter. A wide range of inks including colloidal suspensions and gels, nanoparticle-filled inks, polymer melts, fugitive organic inks, hydrogels, sol-gel, and polyelectrolyte inks have been processed using direct-write assembly. Lewis et al. have reached to minimum feature sizes ranging from 250 nm for sol-gel inks and 200 μm for ceramic colloidal inks. Writing of some inks such as polyelectrolyte inks need to be performed into a reservoir-induced coagulation to enable 3D printing, whereas some other inks such as sol-gel inks can be directly printed in air providing excellent control over the deposition process (e.g., the ink flow can be started/stopped repeatedly during assembly).

Figure 11 depicts TE scaffolds with different rod widths, pore size, and materials have been made by the authors using two processes with and without material melting, namely, FDM and solvent-based extrusion freeforming techniques.

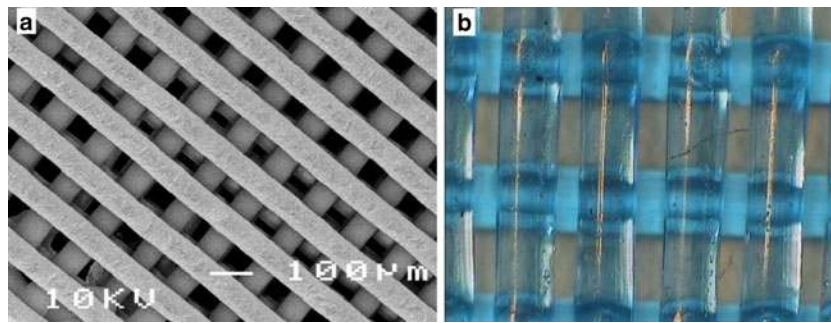


Fig. 11 **a** Plane view of HA scaffold with rod width of 70 μm produced by solvent-based extrusion freeforming. Bioceramic scaffolds produced by solvent-based extrusion freeforming have the finest rod width among other extrusion-based SFF techniques such as direct-

write assembly orrobocasting. **b** PLA scaffold with micropores fabricated using screw-feed FDM system, rod width of 250 μm and air gaps are 100 μm

3.6 Laminated object manufacturing process

LOM system uses laser beam to cut out expected profiles from sheet, provided from an uninterrupted roll, which create final-part layers. Layers stick together by applying a heat-activated plastic which is plated on one surface of the paper and final part [123]. This additive process has several limitations (mainly resolution) for micropart fabrication and is not a potential method to be used in a true 3D microfabrication area. This method is currently used for fabrication of ceramic structures with microscale internal cavities and channels favorable for microfluidic devices. Computer-Aided Manufacturing of Laminated Engineering Materials (CAM-LEM, Inc., USA) has developed special micro-LOM process known as CAM-LEM process. In CAM-LEM process, slices are produced by laser cutting metal tape or sheet of green ceramic. Next, the slices are stacked accurately to create the part. Afterward, the layers are bonded together by applying heat and pressure. The green part is then put into furnace to obtain sufficient strength. Five kinds of materials with different thicknesses can be automatically utilized into a build process. One or more of the materials may work as support materials. Support materials enable the process to build overhangs and internal microvoids/microchannels. The support materials are taken away by using thermal/chemical methods. The main drawback of the process is a large amount of shrinkage (12–18 %) due to thermal post-processing which can lead to dimensional inaccuracies [82]. Layer thickness can range from 30 to 1,300 μm or more, although most common materials are between 150 and 600 μm . CAM-LEM process enables the creation of high-performance microfluidic devices made from ceramic or metal. These provide much better chemical resistance and strength than plastic or silicon, better strength than glass, and high-temperature resistance. CAM-LEM process can be used for fabrication of microsensors, miniature diagnostic devices, lab-on-a-chip, microreactors and heat exchangers, and microfuel cell components.

4 Key 3DDW processes

LCVD, FIBDW, and nozzle dispensing systems are the key 3DDW techniques. Nozzle dispensing systems such as direct-write assembly, PAM, etc were discussed earlier in section 3.5 along with FDM process. In the following section two DW processes, namely, LCVD and FIBDW would be described.

4.1 Laser chemical vapor deposition process

LCVD is a 3DDW process that employs laser beam to convert gaseous reactants into thin solid layers in a selective manner. In LCVD process, laser beam is focused to a spot ($\sim 1 \mu\text{m}$ in diameter) via optical microscope lens and gaseous reactant comprising the materials to be laid down is fed into a build chamber. The substrate is heated selectively by scanning the laser beam over it at usually 0.5–5 mm/s speed to dissociate the reactant gas selectively; consequently, a thin layer of the material is set down onto the substrate. In this way, by repeating laser scan, expected microcomponent can be made layer by layer. There is a possibility to fabricate multimaterial and gradient 3D microstructures by feeding different gases into the build chamber at different times or using a blend of gases with desirable concentrations. Researchers at the Georgia Institute of Technology developed a LCVD system which uses jets of gas to provide a local gaseous atmosphere instead of feeding gaseous precursor materials into the build chamber [82].

Various microparts from variety of ceramics and metals can be produced by LCVD process using different reactant gases. Furthermore, LCVD process can be used to build carbon fibers and multilayered carbon structures. Duty et al. [64] deposited various materials including carbon, silicon carbide, boron, boron nitride, and molybdenum (Mo) onto various substrates including graphite, grafoil, zirconia, alumina, tungsten, and silicon using the Georgia Tech's LCVD system. In 1994, 3D aluminum oxide (Al_2O_3) rods of 3–20 μm diameters were fabricated by Lehmann and Stuke

using LCVD process with growth rate of up to 80 $\mu\text{m/s}$. They used a special blend of trimethylamine alane ($(\text{CH}_3)_3\text{N.AIH}_3$) and oxygen as gas precursor and two orthogonal argon laser beams with 0.2–20 mW power and spot diameter of 3 μm was used instead of a single laser beam [147]. Wanke et al. [256] employed the process with growth rate up to 100 $\mu\text{m/s}$ to fabricate 3D photonic microparts from Al_2O_3 and the technique was later employed by Stuke et al. [227], for fabrication of 3D microelectrical cages to snare microparticles. William et al. [257] utilized LCVD process to fabricate carbon 3D microcoils using ethylene gas precursor. Figure 12 shows a sample Al_2O_3 3D microstructure produced by LCVD process.

A number of factors such as laser beam diameter, energy density, and wavelength as well as substrate thermal properties influence the resolution of this process [82]. Also, the deposition rate is contingent upon the process parameters such as scanning speed, gas pressure, and laser power density. Increasing in gas pressure of the precursor materials and laser power density results in linearly increase of deposition rate. Also, scanning speed is inversely proportional to the deposition rate [257] and the grain size increases with deposition thickness, as reported by Foulon and Stuke [77]. Deposition thickness can be estimated by the equation offered by William et al. [257], for a Gaussian beam profile:

$$h(v_s, t) = \frac{R_0 r t \sqrt{\pi}}{\sqrt{\pi} r + 2(v_s t)}$$

In this equation, r is the laser spot radius, $h(v_s, t)$ is the deposition layer thickness, R_0 is the diffusion-limited axial growth rate, v_s is the scanning speed, and t is process time.

4.2 Focused ion beam direct writing

The principle of FIBDW is similar to LCVD process barring that FIB is employed instead of laser beam for deposition. In this process, a FIB generated from a liquid gallium source is scanned over a build substrate in the presence of gaseous precursors and as a result solid materials are deposited onto

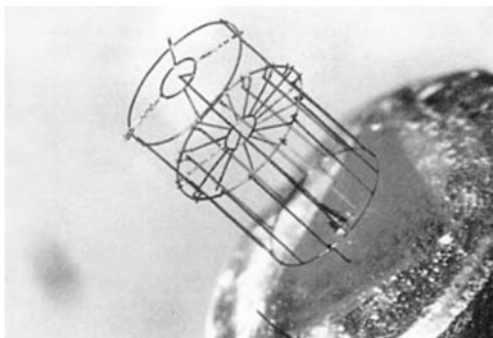


Fig. 12 Aluminum oxide 3D microstructure produced via LCVD process (photo, MPI-Göttingen, Germany, taken from [81])

the substrate [95, 155]. As compared with LCVD, FIBDW has lower deposition rate (normally, 0.05 $\mu\text{m}^3/\text{s}$) but also offers higher resolution. Energy of the ion beam is usually between 10 and 50 keV, with beam currents changing between 1 pA and 10 nA. The minimum deposition thickness is about 10 nm for microstructures with the minimum feature size of 80 nm and aspect ratios between 5 and 10 [185]. Since organometallic mixtures are utilized in FIBDW, metal layers deposited are not pure due to Ga^+ ions and organic impurity [67]. Reyntjens and Puers utilized $\text{W}(\text{CO})_6$ as an organometallic precursor gas for deposition of W [205]. Different microstructures have been fabricated from conductors, such as gold (Au), Al, copper (Cu), Mo, and Pt and insulators, such as TEOS, TMCTS/ O_2 , and PMCPS/ O_2 using different gases [29, 68, 272]. FIBDW is a slow process, so it is usually employed for repair work and low-volume production [184]. In particular, this process can be used for fabrication of 3D microstructures which are utilized for hermetic encapsulation in microsensors [96]. It should be noted that electron beam can also be utilized to induce CVD in a similar way to FIBDW and LCVD. Both electron beam CVD and FIBDW have a better resolution than LCVD, but electron beam CVD is a slower process as compared with LCVD and FIBDW [21].

5 Key hybrid process

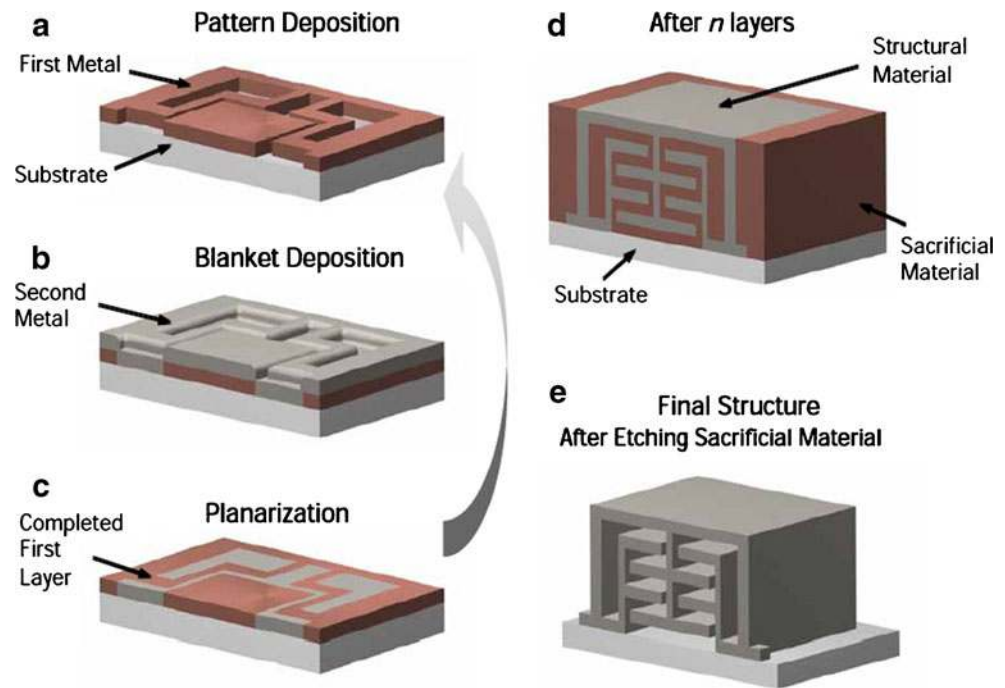
Two processes namely, EFAB and SDM are subset to this group. Only EFAB process has been discussed in this section since to date SDM has not shown applicability for true 3D micromanufacturing.

5.1 Electrochemical fabrication process

The EFAB is a hybrid process for volume manufacturing of microdevices with features as small as 20 μm and tolerances of $\pm 2 \mu\text{m}$ with no assembly. EFAB process is a trademark of Microfabrica (formerly MEMGen Corp.) and is based on multilayer electrodeposition and planarization of at least two metals: one structural material and one sacrificial material [48]. Figure 13 shows the EFAB process schematically.

The EFAB is a hybrid (additive/subtractive) process in which three-step process is used to generate each layer. This three-step process is repeated to build the desired complex microdevices layer by layer. The three-step process in each layer includes: structural material electrodeposition, sacrificial material electrodeposition, and planarization, respectively. Both materials are deposited by electroplating, and one (sacrificial material in Fig. 13) is deposited using a special selective electroplating process called “instant masking.” The EFAB process begins by electrodeposition of sacrificial material using instant masking. Using instant

Fig. 13 The EFAB process [27]



masking, a negative micromold is generated by custom photolithography process in which a precise thickness of photoresist is exposed to the UV light selectively through photomask to generate a pattern. The produced micromold is placed into an electrodeposition to deposit sacrificial material (Cu). The photoresist is then chemically removed and the structural material is deposited into the area where the photoresist was removed. The structural material fills in the gaps between parts on each layer. Then, both the sacrificial and structural materials are planarized to the same level, establishing the desired layer thickness (2–25 μm). All sacrificial material is etched from the wafer and removed from the devices. There is a possibility to achieve microfeatures up to 20 μm with 2 μm accuracy and repeatability by the EFAB process. Limited materials have been developed by Microfabrica, including: Valloy-120, a nickel–cobalt (Ni–Co) alloy that has mechanical properties that are similar to medical-grade stainless steel; Edura-180, an electroplated rhodium (platinum (Pt) group metal) formulation that is almost as hard as ceramic and has high electrical conductivity; and biocompatible noble metal palladium. Valloy-120 is used as the primary structural material and is an electroplated, fully dense, ductile, corrosion-resistant metal with great mechanical properties and biocompatibility for short time exposure to tissue. Edura-180 is usually used where extreme hardness or wear resistance is required in thin walls. Noble palladium is also served where excellent biocompatibility is required. Properties of commercially available EFAB materials compared with some commonly used medical materials can be found in Cohen et al. [46]. The EFAB process is an ideal approach for producing robust

micrometal parts, subassemblies, and 3D micromachines. This process has a wide range of applications in microindustries, including probes for semiconductor testing, microfluidic devices, minimally invasive medical instruments and implants, high accuracy probes for testing memory chips and microprocessors, inertial sensing devices, military fuzing, and millimeter wave components [46]. Figure 14 shows two 3D microstructures/assemblies produced by the EFAB process.

6 Impacts, applications, and future trends

6.1 Impacts of 3D micro-AM technologies

MEMS processes are silicon-based manufacturing processes (including bulk and surface micromachining), soft lithography, and LIGA process. In silicon bulk micromachining processes, a silicon wafer (or other crystalline materials) is etched, typically anisotropically, to form structures. In silicon surface micromachining processes, layers of polycrystalline silicon are deposited to form structures, typically with oxides deposited as a sacrificial material. Finally, in the LIGA process, a thick polymer layer is exposed to hard X-ray radiation from a synchrotron to define apertures in which are then deposited a metal such as Ni or Cu. To date, silicon micromachining approaches have had great effect on growth and development of microproducts such as sensors but they still have some considerable drawbacks that are obstacles for emersion of new microproducts and have limited silicon micromachining applicability to some

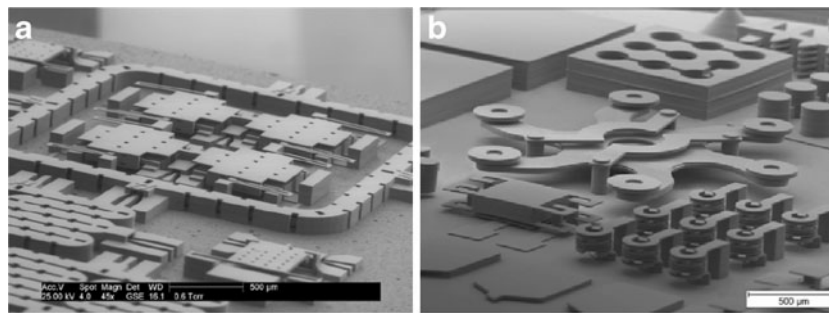


Fig. 14 **a** Hybrid couplers and RF switches for millimeter-wave systems [38]. **b** Different microstructures, including: a fluid injector architecture, fluidic wells and channels, an array of helical inductors,

electrical resistance structures, an accelerometer with capacitive sense plate, geometries for plastic micromolding and embossing, produced from electroplated nickel in 24 layers using EFAB process [43]

commonly used components such as diaphragms, cantilever beams, etc. Moreover, silicon micromachining is an expensive, inflexible, high-risk, and time consuming approach where new microproducts need to be developed. 3D micro-AM technologies provide many benefits as compared with conventional silicon micromachining technologies. The most significant advantage of 3D micro-AM technologies is the aptitude to fabricate true 3D components/structures. Prior to micro-AM technologies, designers have been compelled to take into consideration the limitations of silicon micromachining that is intrinsically planar when designing MEMS/MOEMS devices. In many cases, this limitation is an obstacle to achieve optimum performance of microproducts. Hence, adding 3D capability to design can open up new application areas and solves problems that have hindered MEMS/MOEMS industry. Table 3 shows some examples in which 3D micro-AM processes can be applied to fulfill performance requirements that would be unobtainable using conventional planar techniques.

Using 3D micro-AM processes, microstructures can be fabricated thin where flexibility is required and thick where rigidity is required. Unwanted vibration modes can be eliminated, proof masses can be increased in size, electrodes and shielding can be placed in optimal locations, and systems can be designed with more degrees of freedom and greater functionality [43]. Also, micro-AM processes makes possible an unprecedented level of device complexity, including the creation of fully assembled mechanisms with multiple independent, moving parts which can avoid the need for costly microassembly [49].

As a consequence of what was discussed above, 3D micro-AM processes enables new types of designs previously impossible to produce while offering cost reduction on specific types of microdevices. Silicon technology has still a justification for its existence and is still a preferable approach in many cases in terms of cost, time, functionality, and reliability. Silicon technology has shown its success in many different applications, and currently micro-AM technologies can be an effective tool when there is complexity. In fact, choosing

silicon technology or micro-AM technology would be a debatable issue only if microproducts have complexity. It is believed that micro-AM technologies need more improvement in terms of cost and reliability to broaden their fields of applications. Popularity of silicon in MEMS/MOEMS is mainly due to its mechanical properties. Silicon is a semiconductor which has mechanical properties similar to ceramics such as corrosion resistance, high strength, and no plastic yielding or fatigue behavior at moderate temperatures. In particular, single crystal silicon is an ideal choice for resonant microsystems that need high-Q resonant characteristic and very long cycle life. Therefore, micro-AM technology should be able to live up to material-related reliability expectation to become a standard tool in the micromanufacturing area in the future.

Choosing the right 3D micro-AM process to be used needs a comprehensive knowledge on capabilities and limitations of each process. A comparison of 3D micro-AM systems has been presented in Table 4. Figure 15 graphically compares 3D micro-AM processes and various conventional micromanufacturing methods as well as some important MEMS manufacturing processes in terms of complexity and feature size.

As seen in Fig. 15, conventional fabrication technologies such as bulk micromachining and polysilicon surface micromachining are still preferable approaches for structures with rather low intricacy. But for components with high complexity, micro-AM processes are more favorable. It should be noted that for microproducts with very high intricacy EFAB is the best solution among micro-AM processes that can fulfill device assembly.

Silicon is not the ideal material for every application since it is very brittle and tends to fail unexpectedly and calamitously at high loads (e.g., shock and vibration). For this reason, protecting silicon from surrounding environment is one of the most significant challenges in silicon microproduct packaging. Thus, utilization of 3D micro-AM processes for fabrication of microproducts from different robust materials which have less severe packaging requirements can be an efficient measure to solve packaging problems. Most of micro-AM systems are able to produce

Table 3 MEMS component design using 3D micro-AM processes and conventional planar micromanufacturing techniques (reproduced from [43])

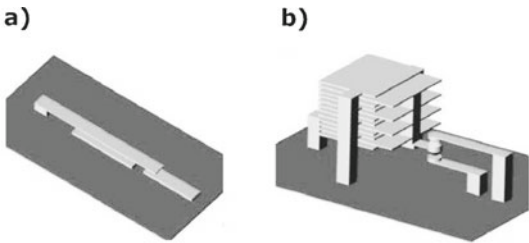
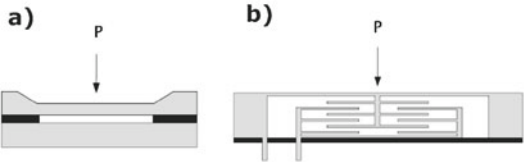
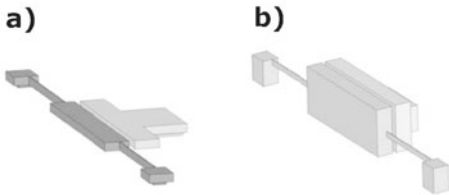
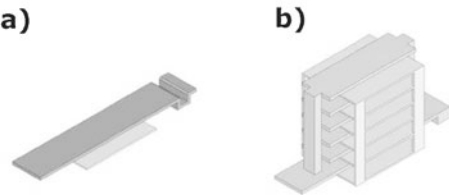
Design examples	Description
	<p>MEMS switch: a) Design for manufacturing with conventional planar micromanufacturing approaches b) Design for manufacturing with 3D micro AM processes</p> <p>In the conventional approach (a), a cantilever beam is suspended above the substrate, and is driven by electrodes on the substrate to contact another electrode on the substrate to close a circuit. There is a fundamental trade-off between the drive voltage and isolation of a MEMS switch. That is, increasing the gap between the suspended beam and the substrate improves isolation at the cost of increased drive voltage. However, this trade-off is based on the assumption that electrodes must lie flat on the substrate (a planar assumption). With 3D micro AM technologies, there are more optimal ways to place drive electrodes, for example by coupling the beam separately to a set of stacked electrodes (b). The design using 3D micro AM processes provides improved isolation, reduced drive voltage, and double-throw functionality.</p>
	<p>Capacitive pressure sensor: a) Design for manufacturing with conventional planar micromanufacturing approaches b) Design for manufacturing with 3D micro AM processes</p> <p>A silicon capacitive pressure sensor (a) is typically comprised of two micromachined and bonded silicon wafers. The die must be protected in an external package. With 3D micro AM technologies (b), it is possible to fabricate a metal diaphragm pressure sensor which provides a substantially larger sense capacitance using stacked electrodes, as well as self-packaging and improved media compatibility.</p>
	<p>Gap Closing Actuator: a) Design for manufacturing with conventional planar micromanufacturing approaches b) Design for manufacturing with 3D micro AM processes</p> <p>Larger forces for gap closing actuators can be realized by increasing the actuator height using 3D micro AM processes since there is no limitation in height of microparts.</p>
	<p>Gap Closing Actuator: a) Design for manufacturing with conventional planar micromanufacturing approaches b) Design for manufacturing with 3D micro AM processes</p> <p>Larger forces for gap closing actuators can be realized by increasing the number of actuator layers.</p>

Table 4 Comparison of the key micro-AM systems

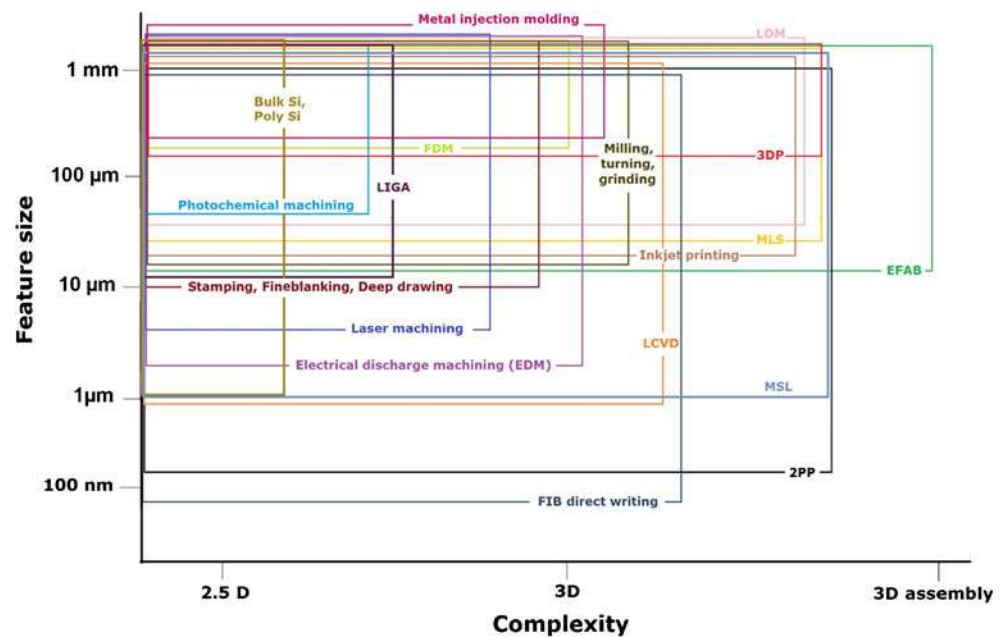
Process	Strengths and weaknesses	Resolution (μm)	Materials	References
MSL	Complicated, yet well-understood and proven technology, high-resolution, suitable for volume production, suitable for true 3D microparts, high repeatability, and limited materials	2	Photocurable polymers; hydrogels; ceramics—PZT, alumina, and HA; and metals—WC, Co, Al, and Cu	[9, 51, 82, 139]
MLS	Ability of multimaterial sintering, no support structure needed, suitable for true 3D microparts, facilities are required to provide fine powders and post-processing microparts have porosity, and high-temperature process	30	Metals—Ag, Cu, and Al; ceramics; molybdenum; and 316L stainless steel	[200, 203, 226]
3DP	Ability of multimaterial printing, suitable for volume production, suitable for real 3D microparts, low-temperature process, no support structure needed, low surface-quality microparts have porosity, and achievable minimum feature size limited to 200 μm	20	Metals and ceramics	[111, 113]
Inkjet printing processes	Wide range of materials, ability of multimaterial printing, ability of writing in 3D space, ideal for deposition of biological inks noncontact easy material handling, sensitive process, fair repeatability, and support structure is needed for 3D microparts	20	Liquid with viscosity of 2–10 mPas (can contain small particles (CIJ)) and liquid with viscosity of 10–100 mPas (can contain small particles (DOD))	[82, 96]
FDM	Easy process, ability of multimaterial deposition, low repeatability, high operating temperatures, commonly is used for microstructure fabrication, and limited biological materials (in order to process high temperature)	200	Thermoplastics	[82, 258]
LOM	Suitable for microceramic parts; fully dense microstructure (>99 %); high mechanical strength; internal, hollow-shaped cavities and channels; part shrinkage after post-processing; achievable minimum feature size limited to 80 μm ; and post-processing facilities are required	50	Ceramics—alumina, silicon nitride, and zirconia and metals—316L stainless steel	[82]
FIBDW	High-resolution process, ability of nanofabrication, favorable for 3D fabrication, slow process, and sensitive process	80	Metals and insulators	[82, 96]
LCVD	Multimaterial is possible; high-resolution process, low-deposition rate, and high-system complexity; high-temperature deposition; and controlled-atmosphere chamber is required	1	Metals and semiconductors	[82, 96]
EFAB	Highly robust microparts, suitable for true 3D microparts and complex mechanisms without the need for assembly, favorable for medical devices, devices cannot be too large and have limited height (1.25 mm), and complete removal of sacrificial material is difficult in some cases	20	Valloy-120 (Ni–Co alloy), Edura-180 (electroplated Rh), and palladium	[27, 46, 48]

MSL micro-stereolithography, *PZT* lead zirconate titanate, *HA* hydroxyapatite, *WC* tungsten carbide, *Co* cobalt, *Al* aluminum, *Cu* copper, *MLS* microlaser sintering, *Ag* silver, *3DP* 3D printing, *CIJ* continuous inkjet, *DOD* drop-on-demand, *FDM* fused deposition modelling, *LOM* laminated object manufacturing, *FIBDW* focused ion beam direct writing, *LCVD* laser chemical vapor deposition, *EFAB* electrochemical fabrication, *Ni–Co* nickel–cobalt, *Rh* rhodium

microparts from a variety of metals which have many useful properties such as high electrical and thermal conductivity, greater fracture resistance than silicon, high reflectance, high temperature stability, and magnetic properties. Fatigue is the most significant disadvantage of metals for MEMS/MOEMS devices as compared with silicon. Nevertheless, several high-cycle resonant devices have been

produced from metals instead of silicon such as Texas Instruments' DMD which is used in projection MSL systems as discussed in Section 3.1. It is believed that fatigue effect can be controlled in microsystems produced from metals if microproduct is designed appropriately for remaining cyclic operating stresses within elastic boundaries.

Fig. 15 Comparison of micro-AM with conventional micro-manufacturing processes (data for conventional microfabrication processes from [44, 155, 197, 199])



Despite what were mentioned as advantages of 3D micro-AM process, there are still some aspects that should be improved. The layered nature of 3D micro-AM processes results in stair-step effect in micropart surfaces, as well as inter-layer misalignment problem in some 3D micro-AM systems. In addition, layer manufacturing also produces anisotropic mechanical properties, although in most cases the anisotropy is not significant and can be neglected. Furthermore, high productivity, easy handling, finishing, and post-processing of the microparts should be possible for cost-effective micromanufacturing (small series to mass production). Currently, none of the micro-AM processes fulfill all the requirements, and suitable micro-AM technology should be selected for a specific application. On the other hand, reliability is one of the most significant aspects for commercial microproducts, and a systematic reliability study on microproducts produced by 3D micro-AM technologies should be conducted to acquire more knowledge on current limitations and requirements and further improvements. Reliability-related material properties such as fatigue and strength are very important, and 3D micro-AM processes should be able to fulfill this significant feature.

6.2 Applications, challenges, and further improvements

Major challenges for 3D micro-AM are process modeling, development of new mechanisms and optimization, merging problems for microdevice applications, and appraisal of functional performance of 3D microstructures. 3D micro-AM processes will play an important role and will provide a new idea in tendency of this technology by growing progression in micro/nanosystems combining microfluidics, optical functions, biological, and electronics.

Some general improvements should be considered in 3D micro-additive processes. First of all, more advancement in layer binding, resolution, and surface finish of produced 3D microstructures would be advantageous. Also, deeper comprehending about 3D micro-additive processes is needed to discover and develop more quantitative relationships between effective process parameters. In this way, more trustworthy process modeling with more accurate results will be developed which cause optimization of 3D micro-additive processes. For this aim, more quantitative information about physical properties of the materials used by 3D micro-AM technologies should be obtained by using measurement techniques.

6.2.1 MSL process

Microstereolithographic processes have shown their efficiency in true 3D microfabrication area, but there is still demand for more improvements in materials for MEMS/MOEMS industries. To date, different components have been fabricated via polymerization of some advanced functional material suspensions such as liquid crystalline polymers with high stiffness and thermal stability [25, 247, 248]; ceramics including silica, silicon nitride, alumina [16, 110, 183, 195, 196, 249, 275, 276], hydroxyapatite [6, 93, 173], and lead zirconate titanate [51]; and metals including: Al, Cu [139], tungsten carbide, and Co [10, 80]. SL of ceramic or metallic materials needs a UV-curable suspension prepared with a prepolymer that will act as the binder material, a photoinitiator, ceramic or metallic powder, and additives [9, 62]. Hydrogels composed of synthetic polymers, natural polymers, or combination of both natural and synthetic polymers can be used in stereolithographic applications [75, 158,

213]. Fabrication of 3D cell matrix structures with micro-scale resolution has been reported by Liu and Bhatia [154] via multiple steps of micropatterned photopolymerisation processes.

There are several domains of applications for the MSL process, such as microrapid prototyping of mechanical components, medical microprobes with embedded optical and chemical sensors [13]; hearing-aid microcomponents; passive microfluidic components, such as microconnectors [18], microvenous valve [103], microfluidic channels [126], and 3D micromixers [14, 15, 120]; and active microfluidic components such as micropumps (Fig. 16b) [1, 33, 101, 102], valves, and active micromixers by combining with piezoelectric actuators or SMA components [91, 106]. In addition, there is a possibility to combine MSL process with other conventional silicon-based micromachining technologies. Bertsch et al. [17, 18] combined MSL with LIGA process to add capabilities of LIGA process (e.g., wafer-level processing and smooth and vertical walls) to those of MSL (e.g., complex true 3D shapes) (Fig. 16a). Takagi et al. reported fabrication of a special microclamping tool by construction of a polymeric component using MSL process on top of a piezoelectric actuator [236]. SMA wires can also be inserted in microstructures made by MSL process to produce advanced microactuators having multiple degrees of freedom [9]. Functional microcomponents and sensors can be produced on silicon wafer via conventional planar micromanufacturing approaches and then immerse into the resin bath of a MSL machine for in situ packaging [245, 246]

2PP microfabrication has submicrometer resolution and is a suitable alternative to produce 3D photonic crystals which can work in the near-IR spectral range [57, 214, 224]. 2PP microfabrication has the capability to build arbitrary components and 3D photonic crystal as compared with conventional approaches [58, 78, 137, 223, 239] (Fig. 4a). Of particular interest are waveguides [122], diffractive optics and refractive micro-optical elements [87], and plasmonic components [204]. Maruo et al. [169] reported fabrication of optically actuated micromechanical systems for cell manipulation and microfluidic systems applications. To date, different techniques for metallization of fabricated components by 2PP process from photosensitive materials

that are intrinsically dielectric have been presented [76, 181]. A variety of microelectronic structures, such as microinductor coils can be realized using such metallization approaches [74]. Concerning on medical applications, 2PP can be applied for the fabrication of medical micromechanical systems [231], scaffolds for TE [209], 3D microstructures with nanostructured surfaces to investigate cell behavior [211] (Fig. 4b), and biomedical devices [60]. In 2011, Bastmeyer's group attained to cultivate cells on 3D structures produced by 2PP process in a specific manner. The most significant achievement is that the cells are offered small "holds" in the micrometer range on the scaffold, to which they can adhere. Adhesion is possible to these holds only and not to the remaining structure. For the first time, cell adhesion and, hence, cell shape are influenced precisely in three dimensions (Fig. 17) [121].

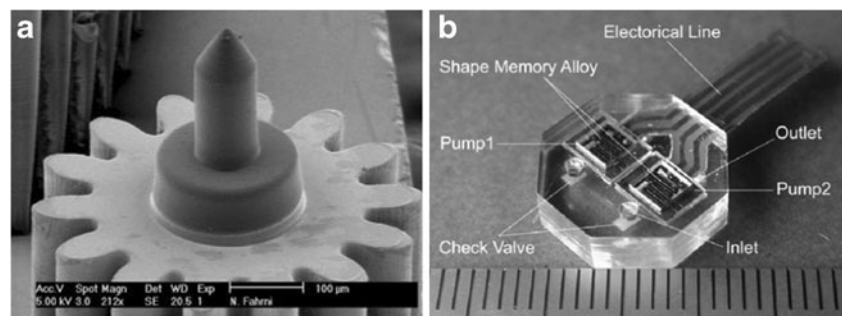
Beside the mentioned capabilities of the 2PP process, it is still a process under research and development and is not being used efficiently in micromanufacturing industry for producing real products since it is a very slow process.

It is believed that the MSL process is the most favorable AM technology for microfabrication due to high resolution, good surface quality, and no porosity. However, the most important challenge for microstereolithographic processes is materials, as demand for fabricating complex microstructures from a wide range of materials especially semiconductor materials is observed. Further improvements are still necessary in the field of material (adjustable mechanical and optical properties, water resistance for microfluidic devices, and biocompatibility for medical devices) and cost-efficiency.

6.2.2 Inkjet printing processes

To date, microfabrication of polymeric true 3D microstructures using inkjet printing processes has been demonstrated. The ability of inkjet printing technology to produce micro-parts from a wide range of materials including optical polymers, solders, thermoplastics, light-emitting polymers, organic transistor, biologically active fluids, and precursors for chemical synthesis has been demonstrated. Inkjet printing process is mainly employed for 2 and 2.5D applications

Fig. 16 **a** Conical axle added by MSL on a SU-8 microgear produced already by LIGA process [9]. **b** Micropump chip [101]



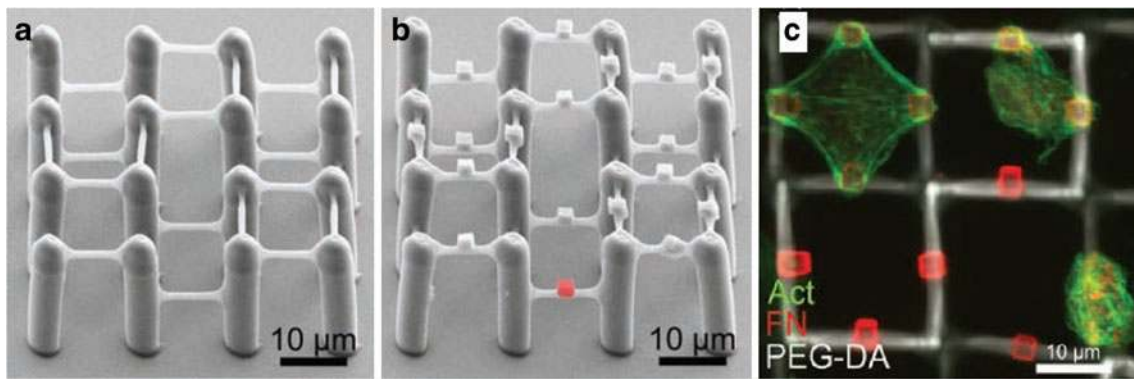


Fig. 17 Cultivating cells on two-component composite scaffold—**a** 3D polymer scaffold from PEGDA/PETA produced by 2PP and **b** composite structure as a scaffold for cells. Cubes made from Ormocomp in red color. **c** Primary chicken fibroblasts adhering

to one, two, or three protein-binding Ormocomp cubes: cytoskeleton of the cell is colored green, parts of the two-component polymer scaffold are colored white, and the “cell holds” are colored red [121]

currently in MEMS/MOEMS systems, such as mask-less printing of electronic circuits on glass substrate using electrostatic inkjet printing [116] and solder printing for IC test boards [152]. Specially, it is a well-established process for printing microlenses and solder bumping (Fig. 18).

Several research works have been performed on fabrication of microstructures and pillars from ceramics such as alumina, zircon, and silicon nitride [3, 31, 56, 65, 70, 149, 189, 237] and metallic microstructures from Cu, Al, tin, various solders, and mercury [30, 152, 153, 194, 262]. More emphasis should be placed on the development of inkjet printing systems which are able to produce high-quality true 3D microcomponents from functional materials, such as metals, ceramics, and smart materials to achieve required thermal, mechanical, and electrical properties for MEMS/MOEMS industry. Figure 19a shows an example of a 3D electric circuit formed from metal and resin. In addition, by distributing jets of different material, 3D functionally gradient structures can be generated as shown in Fig. 19b.

There are still some drawbacks, such as porosity and surface quality of 3D metallic microstructures. To improve ink jetting of 3D metals, Tropmann et al. [244] proposed a

novel pneumatically actuated inkjet printing system composed of a novel star-shaped nozzle that stabilizes liquid plugs in its center by means of capillary forces for the generation of liquid metal microdroplets in the nano- to picoliter range. The StarJet can be operated in two modes: either continuous droplet dispensing mode (Fig. 20b) or drop-on-demand (DOD) mode (Fig. 20a).

There are several points of view for the widely utilized multipurpose inkjet printing processes which need additional research and development. Enhanced modeling approaches for jetting and droplet generation, droplet impact, and drying droplets in each layer would be useful for process optimization. Some inherent restrictions on fluid properties are known which affect droplet generation and break-up, but there is still a challenge to expand domain of fluids which have a capability for microinkjet printing. As an example, deeper comprehending of the printing of non-Newtonian fluids would be beneficial to attain effective inks which have high concentrations of solid particles or polymers. Further development of low-cost conductive materials which can be used in form of an ink by microinkjet printing and are able to attain high and

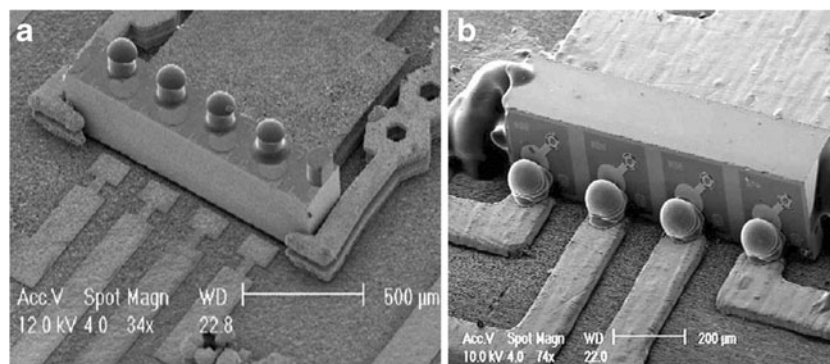
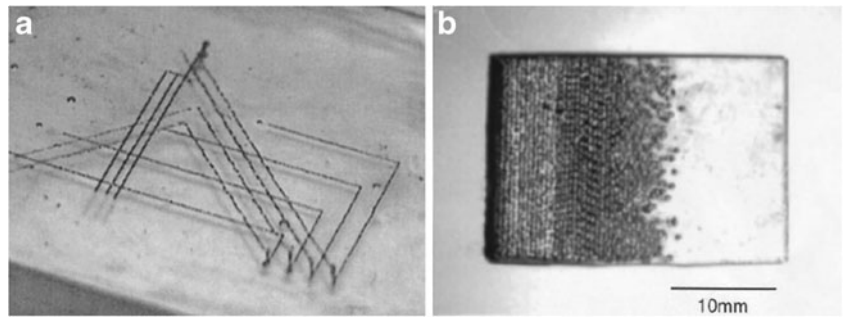


Fig. 18 Printing microlenses and solder bumping. **a** Lensed VCSEL array aligned to the optoelectronic chip using the clammer in the figure. Lenses on top of the posts printed at MicroFab. **b** Solder bumping is noncontact and can be directed at any angle in 3D space to

accommodate unique applications. A 45° rotation of the print head was used to deposit molten solder droplets, 25–125 µm in diameter, at rates up to 400/s to a right angle interface between conductors and a VCSEL array [176]

Fig. 19 **a** 3D electric circuit build from metal and resin and **b** a functional gradient structure made of metal and resin [263]



stable conductivity would be a great advancement in this area. Also, the applications of microinkjet printing in 3D microfabrication will expand with emersion of new jetting techniques such as electrostatic and better understanding of the process and utilization of efficient modeling techniques.

In the future, both the number and type of products fabricated using inkjet technology should increase, and the availability and capabilities of inkjet-based prototyping and production tools should expand. Using inkjet-based methods, commercialization of products is in progress for DNA microarrays, color displays, electronics assembly, and photonic elements. Inkjet printing processes in combination with the printed electronics technology makes it possible to manufacture real MEMS parts [125, 140, 229]. Future works may be focused on fabrication of true 3D high accuracy and improved surface finish part based on tailor made inks, using multi-material printing process. It is believed that using chemically etched able metal as support materials will be a worthwhile attempt toward improvement of fabrication of true 3D metal microstructures. As for ceramics, future works can be concentrated on utilization of inkjet printing in innovative way for manufacturing various components, such as: multilayered ceramics (capacitors, sensors, and actuators), 3D electronic ceramic components (high-temperature cofired ceramic and low-temperature cofired ceramic), and conductive layers on ceramic (photovoltaic components and thick film electronic).

6.2.3 3DP process

3DP process is easily adaptable to a variety of materials systems, allowing the production of metallic/ceramic

microparts with novel compositions. This process currently suffers from some drawbacks such as inadequate surface quality, minimum achievable feature size, and porosity but has demonstrated good applicability for true 3D microfabrication. Both 3DP and inkjet printing processes are based on ink jet technology, but 3DP takes the advantage of using powders as a substrate in each layer and as a result no support material is required for true 3D microfabrication. Moreover, 3DP can be served in indirect routes such as ceramic molds to build microparts from variety of materials. There is also possibility to combine inkjet printing and 3DP process to produce final microproducts. Especially inkjet printing of tailor made inks on the 3D surface produced already by 3DP process can open new opportunities. Figure 21 shows an example of combination of Feubic's 3DP and inkjet printing process to produce final product. Achieved 3D electrical interconnects is one of the most particular issues in microsystem integration. 3D electrical interconnects have always been a challenge in electronics packaging. In this example, inkjet printing of silver (Ag) ink in 3D surface produced already by 3DP process has been successfully demonstrated. Writing in 3D space is also persuaded by other microdeposition processes such as aerosol jet process.

Further researches should be focused on increasing resolution of micro-3DP process and expanding range of materials especially for MEMS application. The feasibility of manufacturing complex Ni–Ti parts by 3DP process has already been studied [157] and appropriate conditions for layer deposition, printing, debinding, and sintering have been established. 3Dprinted Ni–Ti specimens exhibit shape memory behavior [32]. Nevertheless, further researches are

Fig. 20 **a** A microtube with 315- μm wall thickness printed by StarJet system in DOD mode. The close-up view shows the morphology of the porous surface. **b** Coil-like structure printed by StarJet system on a heated rotating substrate in continuous mode (*inset graph, top and side view of the star-shaped nozzle*) [136, 244]

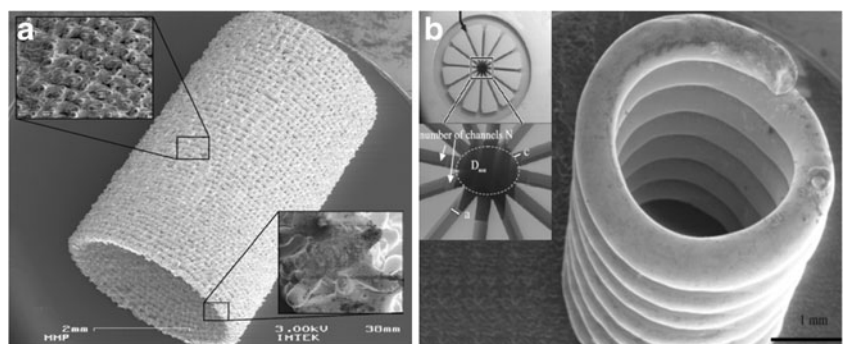
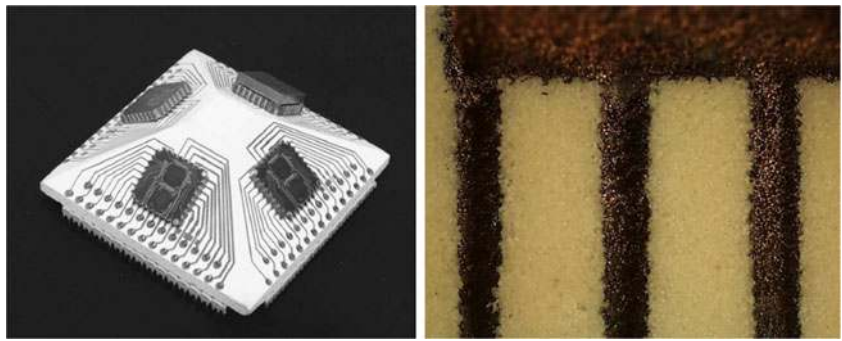


Fig. 21 Ceramic Inertial Measurement Unit with four gyroscopes and circuit patterns. 3DP was used for the ceramic layer manufacturing process, and inkjet printing was used for the printing of silver ink for circuit patterns (silver line, ~300 μm) [112]



necessary to study dimensional stability, and test functionality of Ni–Ti microparts. As a practical case, Walters et al. [254] reported 3D printing of a biologically driven Ni–Ti actuator.

The main challenges of micro-3DP are currently resolution of the process and difficulties in powder recoating and part depowdering in micron size scale. On the other hand, microparts have a rough surface and remarkable porosity. These limitations can be highlighted more for specific applications such as microfluidic devices. It is believed that powder-based processes such as 3DP has little further potential for enhancing the resolution since if the powder size gets smaller and smaller, powder handling (recoating) becomes impossible. Implementation of bimodal powder distribution approach proposed by Lanzetta and Sachs [135] in micro-3DP may be a useful measure to improve surface quality of microprinted parts.

6.2.4 SLS process

SLS process, as a powder-based microfabrication technique, has higher resolution as compared with 3DP process. Different powders such as tungsten, Cu, Ag and tungsten/Cu mixtures, single-phase Mo, and stainless steel alloy 316L have been successfully processed. With a slightly different approach, the technique is also applied for processing of ceramics and composite materials. There are a lot of application areas for microtechnologies, growing constantly. Of particular interest are micromolded parts, microeroding molds and microfluid mixer, microsensors and connectors, endoscopes, minimal-invasive surgery, microimplants, microreactors, microheat exchanger, etc. Nonetheless, MLS needs several improvements to become an efficient approach in microindustry and fulfill different requirements in this area. The key current challenges may be limited materials, powder handling (recoating), part removal/cleaning, surface roughness, and achievable resolution. Concerning on materials, the main challenge facing is finding the process parameters for different materials. Using dry powder dispensing techniques instead of conventional powder recoating can be a good solution to overcome fine powder handling problem. Dry powder dispensing systems

(especially ultrasonic nozzle dispensing systems) have demonstrated their great ability in precise placement of fine powders [159, 264, 265]. So, the authors believe that using such selective powder dispensing mechanism in MLS process may be an efficient measure to solve the problem of fine powder handling and improve resolution of the process as well as adding possibility of lateral material change in multimaterial microparts. Serving such selective dry powder dispensing system integrated with a complete manufacturing line, including laser sintering, part removal/cleaning can be a worthwhile suggestion for further works.

6.2.5 FDM and extrusion-based processes

As mentioned in Section 3.5, FDM and most of extrusion-based processes are currently used mainly for fabrication of TE 3D scaffolds with micron size filaments. Precise control of extrusion is the most important issue for extrusion-based systems (especially processes with material melting) to find their way to other applications. Precision control of extrusion in melt-based extrusion freeforming systems would rely on a significant number of parameters such as input pressure, temperature, nozzle diameter, material characteristics, temperature build up within the part [8]. In the meantime, an appropriate layer filling strategy should be developed since inappropriate fill pattern style can result in unwelcome microvoids inside the microparts. On the other hand, current materials available for extrusion-based systems cannot fulfill the requirements in the fields of MEMS/MOEMS industry. Amorphous polymers have demonstrated more compatibility with melt based, such as FDM process than highly crystalline polymers. Nevertheless, the ability of FDM for fabrication of parts from advanced ceramics that can quickly solidify has been demonstrated in macroscale [107]. Research on materials would be beneficial and can widen the use of extrusion-based systems in microindustries. Impossibility of drawing sharp external corners and anisotropic nature of a part's properties are two other disadvantages of FDM process that should be taken into consideration. Development of a special multinozzle extrusion-based system with the ability of precisely controlling of

extrusion of variety of functional/composite materials would be a worthwhile idea for further studies.

Recently, Schuurman et al. [212] used a hybrid bioplotting approach for fabrication of solid biodegradable material (polymers and ceramics) with cell-laden hydrogels that could combine favorable mechanical properties with cells positioned at defined locations at high densities. Miranda et al. [179] used robocasting process to produce β -TCP scaffolds with designed, 3D geometry and mesoscale porosity using concentrated β -TCP inks with suitable viscoelastic properties. The deposition was done in a nonwetting oil bath to prevent nonuniform drying during assembly. Dorj et al. [61] used robocasting process to produce a novel nanocomposite scaffold made of chitosan and nanobioactive glass (nBG) retaining dual-pore structure. Robocasting was carried out under a cooled bath containing dry ice, to rapidly solidify the scaffold as at ambient conditions, the dispensed solution was hard to solidify. The chitosan/nBG nanocomposite scaffolds were well constructed, with aligned macrochannelled pore structure.

Applications of the solvent-based extrusion freeforming recently include fabrication of electromagnetic crystals [160], electromagnetic bandgap materials (EBG) [141, 161], millimetre-wave antenna [142], metamaterials [143], and carbon scaffold for catalyst support [165]. Dielectric ceramic materials were used including alumina [160], quartz [162], LaO_3 (Mg, 0.5 and Ti, 0.5), and TiO_4 (Zr, 0.8 and Sn, 0.2) [161]. Wide range of filaments diameters from 150 [162] to 500 μm [163] were used for fabrication of EBG with different band gap. The effect of rheological properties of the paste on the shape tolerance was investigated. When the extruded filament spans more than a critical distance, the filament deforms and leads to sagging [164]. Cylindrical woodpile structure has been fabricated for narrow beam azimuthally omni-directional millimeter-wave antenna [145, 146].

In recent years, researchers have focused on extending direct-write assembly process to biomedical applications. Using biocompatible inks, different 3D scaffolds and microvascular networks have been printed for tissue engineering and cell culture. 3D HA scaffolds with 250 μm road width [175, 220], and 3D scaffolds composed of a gradient array of silk/HA filaments at size 200 μm were fabricated by direct-write assembly [233]. 3D microperiodic hydrogel scaffolds composed of 1- [7] and 10- μm [217] rods were produced for guided cell growth by direct writing of a poly (2-hydroxyethyl methacrylate)-based ink through a gold-coated deposition micronozzle that is simultaneously photopolymerized via UV illumination. Biocompatible silk optical waveguides as fine as 5 μm was produced by direct-write assembly of a concentrated silk fibroin ink through a micronozzle into a methanol-rich coagulation reservoir [192]. Figure 22 [2] depicts some microstructures have been produced using advanced extrusion-based systems.

Cell-based printing techniques have also been intensively investigated in recent years and many innovative approaches such as organ bioprinting [180], laser writing of cells [210], bio-electrospraying [108], and biological laser printing [8] have surfaced to complement limitations in scaffold-based tissue engineering. Organ bioprinting is defined as the engineering of 3D living structures supported by the self-assembly/organizing capabilities of cells delivered through the application of AM techniques based on laser, inkjet, or extrusion freeforming technologies [22]. In direct bioprinting, balls or continuous flows of bioinks are deposited in well-defined topological patterns into biopaper layers. The bioink building blocks typically have a spherical or cylindrical shape and consist of single or multiple cell types. In a post-processing step, the construct is transferred to a bioreactor and the bioink spheres are fused. The biopaper, an inert and biocompatible hydrogel, can be removed after construction in post-processing step [22]. Several extrusion-based systems such as 3D bioplotter described earlier can be served as a bioprinter, if sterile conditions can be acquired. However, it should be noted that, technologically, bioprinting using extrusion-based AM techniques is still in its infancy. Different living structures have been produced using hydrogel structures containing viable cells, but the designs have been simple and isotropic, and mechanical properties were not satisfactory [174]. Thus, future works in this area are mainly focused on effective utilization of multinozzle extrusion-based AM systems to produce living macro/microstructures with controlled compositions and improved accuracy.

6.2.6 LCVD process

LCVD system has been applied for deposition of variety of materials such as carbon, silicon carbide, boron, boron nitride, and Mo onto various substrates including graphite, grafoil, zirconia, alumina, tungsten, and silicon [64]. Wide range of materials and complexity of microparts are the most significant advantages of LCVD process and make LCVD a viable technology for further developments. Nevertheless, LCVD has a relatively high cost and system complexity as compared with most micro-AM techniques and is a high-temperature process. In addition, microparts are built in a controlled-atmosphere chamber and this limits ability of LCVD process to make deposits on larger pre-existing structures [82]. LCVD is a high-resolution process but no cost-effective production because of long building time. One efficient approach is selective-area laser-deposition vapor-infiltration (SALDVI) technique in which the laser scans and heats the powder bed in a selective manner and solid material created from the gas is applied to bind the heated powders material together [52]. SALDVI is much a faster process than LCVD, but microparts are

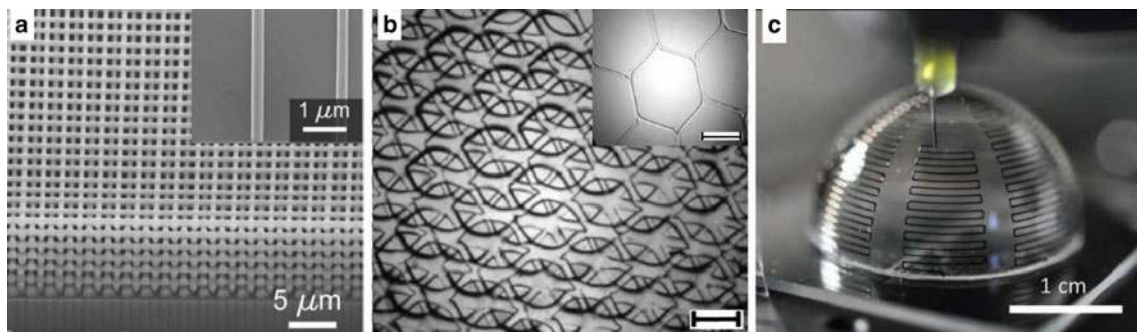


Fig. 22 Different applications of advanced extrusion-based systems: **a** cross-section of highly uniform 3D microperiodic structure with 520-nm rod width fabricated by direct-write assembly process using sol–gel ink based on calcined TiO_2 ; *inset picture* shows single TiO_2 rods as

fine as 270 nm [63]. **b** 3D scaffolds of PLGA produced by PAM process, *inset picture* shows high-resolution 2D hexagonal (scale bars, 500 μm) [31]. **c** Conformal printing of electrically small antennas on 3D surfaces using direct-write assembly of silver ink [2]

composite in nature and may be porous. Further improvements on building speed are necessary for LCVD in order to become cost efficient.

6.2.7 FIB process

As compared with LCVD, FIBDW is a well-established micro/nanofabrication approach. To date, numerous complex micro/nanostructures have been fabricated using FIBDW. Various types of manipulators such as two pillars, 3D-lamented pleats structure, and a nanoactuator with a coil structure were fabricated as shown in [129]. In addition, a nanomanipulator with four fingers was developed, and its performance was tested to catch the target [128, 172]. Various shapes of 3D nanorotors and bionanotools (Fig. 22) using $\text{C}_{14}\text{H}_{10}$ gas have been developed by Matsui's research group [100]. The rotors were fabricated using nanosheet (thickness, 100 nm) by shaping in the free space. The cell wall cutting tool (Fig. 22b) was fabricated on a glass capillary for bioexperiments and medical treatment. Figure 22c shows the filtering tool which has 13 μm of the outer diameter and 7 μm of the inner diameter. It has a needle that penetrates the cell, a retention table to hold the organelles, and a nanonet structure to filter them.

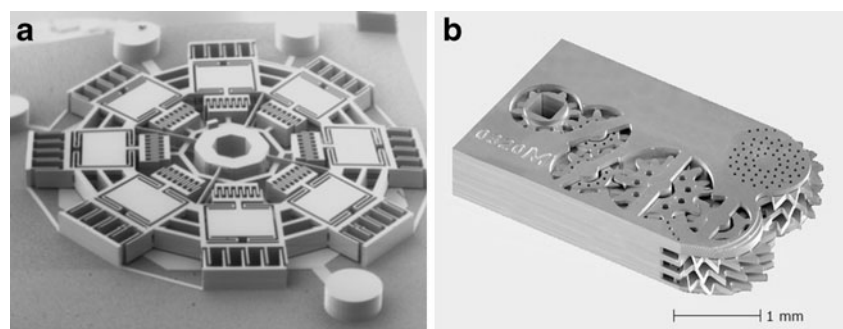
The attempts and developments toward improving FIBDW can be investigated with a number of process parameters including ion dose, dwell time, refresh time,

current density, spot size, ion current, incidence angle, ion energy, overlapping, ion species, and precursor gas [119]. There are still several impediments to overcome the limitations of physical and chemical phenomena in having structural stability in FIBDW. While being extremely accurate and flexible, the method suffers from a very low speed, making it virtually impossible to fabricate large arrays of structures. However, more applications will be tried using FIB's expandable capability to the micro/nanoscale fabrication.

6.2.8 EFAB process

In the medical device space, EFAB is currently utilized for production of minimally invasive surgery tools [45], micro-invasive therapies, microtissue debriders (Fig. 23b), monolithically fabricated articulated biopsy forceps, etc. In the field of semiconductor testing, EFAB process is currently used efficiently for manufacturing composite-compliant pins in which different metals are used in the optimal place to probe multiple integrated circuits in parallel. Compliant pins are contact elements that are great springs with excellent electrical conductivity and must-have high-reliability contacts. A number of applications, such as capacitive pressure sensors, electrostatic actuators (including comb drive and gas-closing actuators) with increased height rather than other conventional approaches, such as LIGA or deep

Fig. 23 **a** Gyroscope [44]. **b** Microtissue debrider (photo, Microfabrica Inc.)



reactive ion etching, and fabrication of robust microstructures (rather than brittle silicon) which are in direct contact with the surrounding environment without any protective packaging have been successfully demonstrated. In addition, this process can be used to create radio frequency (RF) building blocks such as fully coaxially shielded transmission lines, couplers, delay lines, patch antennas, and filters. By combining such structures on a single chip using the EFAB process, it is possible to create sophisticated RF systems on a chip, such as a phased array antenna [43]. One application area with considerable activity is the fabrication of very high-frequency passive components for compact microwave and millimeter-wave radar and communications systems (Fig. 14a). Figure 23a shows a gyroscope produced by EFAB process. Other possible microproducts can be actuators using hydraulics or pneumatics, valves and pumps, cams and followers, and linear and hydrostatic bearings [44].

EFAB process is a fast-growing 3D micromanufacturing technology. In 2010, Microfabrica introduced MICA Freeform as a second generation of EFAB process. MICA Freeform differs from EFAB in terms of materials and design rules: noble metal palladium, which is inert and offers bio- and MRI compatibility as well as radiopacity has been developed and minimum gap around a hinge can be 10 μm which was 30 μm in EFAB. However, there are still some aspects that need to be improved. There are currently limitations for maximum number of layers in a part (maximum of 50 layers), producing a maximum part thickness of about 1.25 mm. Moreover, release holes should be designed for complete removal of support materials where internal channels or multiple components are involved. On the other hand, stair-step effect makes some difficulties in some cases and the gap between moving parts in assemblies cannot be smaller than minimum layer thickness. To date, the ability of EFAB to produce microassemblies that include mechanical elements as well as electrically active components such as capacitive sensors and electrostatic actuators has been demonstrated. Electromagnetism or shape memory-based sensing and actuation systems are also possible and are expected to be developed in the future [44]. The feasibility of fabricating devices using EFAB from Ni-Ti has already been demonstrated. Moreover, there exists some limited experience with palladium-Co, stainless steel, Pt, Au, Ag, as well as higher strength Ni-based alloys [43]. Full-commercial development of any of these metals will require the investment of time and resources. Thus, future development will depend on technical requirements and market opportunities.

6.3 Future trends

Most of the MEMS fabrication methods are adopted from standard IC technology. The most common MEMS fabrication

techniques are: bulk micromachining, surface micromachining, and LIGA. These planar micromanufacturing processes have achieved commercial success in different sectors, such as industrial sensor (e.g., pressure sensors), inertial sensor (e.g., accelerometers and rate gyros), and telecommunications (e.g., compliant structures for fiber waveguide alignment, variable optical attenuators, and cross-connect switches). However, there are still some essential limitations that have slowed the adoption and development of MEMS-based systems using these planar manufacturing processes [115]:

1. The structures created by these processes are inherently limited to 2D (e.g., inch worm and comb drive) or to “2.5D” (e.g., self-erecting mirrors) structures that can be erected from 2D structures. True 3D mechatronics implemented this way requires, often tricky, assembly of multiple 2D MEMS components.
2. The nonrecurring engineering costs such as mask generation are high, and this makes it difficult for emerging companies with comparatively small volumes to deploy the technology.
3. The delivery times are long—often 12–15 weeks—extending the “time-to-money” by stretching design, verification, and validation cycles.
4. The manufacturing processes are not truly scalable. For instant, extending the number of layers in surface micromachining process from four to five layers (extending the height of the machine from 10 to 12 μm) could take months or years due to the impact of thermal cycles during deposition of the fifth layer on the residual stresses in layers 1–4 and the corresponding effect of these residual stresses on layer 5.
5. The packaging cost of these components is high. Integration of planar MEMS with optical components (fiber, array waveguides, etc.) and housing often represents 80 % of the manufacturing cost of a microsystem.

3D micro-AM processes can be considered as a promising alternative to assuage the influence of the above items and bring MEMS/MOEMS technologies a significant step further. In addition to 3D design, the speed of micro-AM processes provides profits to both the microproduct development process and to manufacturing. In particular, microsystems can be prototyped faster and this results in lessening microproduct development time and allowing design iteration and optimization. Serious design modifications can be done midway in the product development process without any change to the microfabrication technology. In addition, micro-AM systems can be applied directly for final microproduct manufacturing. In this way, “rapid micro-manufacturing” as a new terminology in micromanufacturing field can be more accessible using 3D micro-AM technologies. Micro-AM processes have shown their

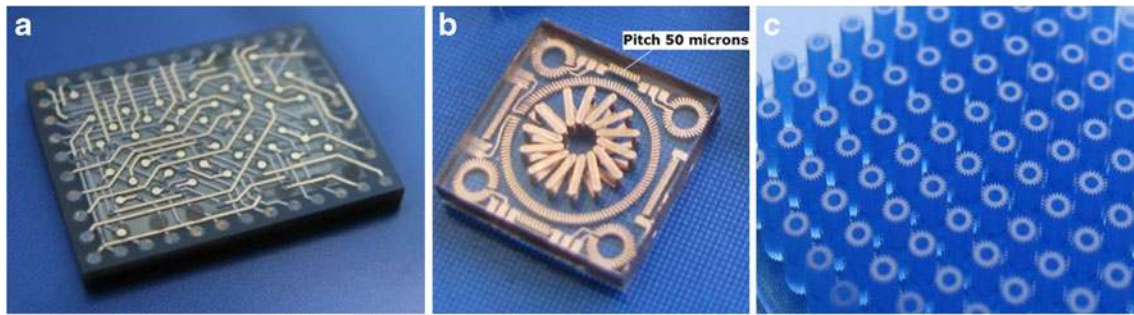


Fig. 24 **a** Complete 3D-CSP-based transceiver module in smallest space ($5.2 \times 5.2 \times 2.2 \text{ mm}^3$) for wireless solutions, **b** 3D-coil variations with RMPD and 3D-CSP for wireless energy supply and

communication, **c** high-volume-production of plastic microgears using RMPD technology, diameters at 828 and 1,200 μm [177]

high potential for RM in microscale due to some significant aspects such as cost efficiency for individualized or small series production and no need to mask preparation like conventional lithographic-based processes, etc. Thus, particular emphasis in the future will be placed on improving 3D micro-AM systems and integration of manufacturing and the packaging/assembly processes to reach the concept of rapid micromanufacturing. MSL is currently the most favorable process among other micro-AM technologies for this goal. MicroTEC is a recognized company with the scope of shifting toward rapid micromanufacturing using MSL process and has demonstrated interesting results in this way. MicroTEC's RMPD technologies are currently used for rapid micromanufacturing of serial parts (1,000–5,000 and more parallel) in variety of materials like plastic or sol-gel. MicroTEC's unique 3D-CSP technology is used to integrate, interconnect, and protect bare dies or other microelectronic elements to get a complete multifunctional system. No wire bonding is needed; interconnection is realized by microstructured metal layers; 3D ultrahigh-density integration is possible; and cooling channels can be integrated to cool hot spots [83]. 3D-CSP technology in combination with RMPD makes an efficient rapid micromanufacturing approach which is applied for many applications, such as life science (e.g., lab on a chip microfluidics), sensor technology (e.g., food control solutions), consumer electronics (e.g., very slim connectors for smart carts), micromechanical parts for metrology tools, etc. Figure 24 shows examples of microTEC's RMPD and 3D-CSP applications in rapid micromanufacturing of plastic parts and microsystems.

Today, markets are looking for energy efficient, fast, and flexible approaches, so conventional micromanufacturing processes are not efficient tools in today's micromanufacturing. Prosperity in new applications will increasingly depend on understanding the strengths and weaknesses of a variety of micro-AM fabrication approaches and using the right fabrication technology or combination of technologies for a given set of requirements. As a consequence of what was

discussed above, it is believed that future works will be mainly concentrated on making micro-AM processes more favorable for rapid micromanufacturing through improving processes and integration of fabrication with assembling and packaging.

7 Conclusions

Many techniques have been developed up to now to respond the demand for high-quality 3D microcomponents used in MEMS and microengineering areas. The additive processes have been identified as a progressive and effective 3D microfabrication technology during two decade evolution. This paper presented a review on the key micro-AM processes used to build functional and true 3D microstructures. The micro-AM systems have been continuously enhanced but more studies are still required to improve the micro-AM systems and the quality of the 3D microstructures. Among micro-AM systems, MSL and EFAB processes have demonstrated more acceptable results in 3D microfabrication area as compare with other discussed systems.

Acknowledgments The authors would like to thank Mr. Urban Harrysson of Fcubic AB and Mrs. Andrea E. Reinhardt of microTEC GmbH for contributions in the preparation of this paper.

References

1. Accoto D, Carrozza MC, Dario P (2000) Modelling of micro-pumps using unimorph piezoelectric actuators and ball valves. *J Micromech Microeng* 10:277–281
2. Adams JJ, DUOSS EB, Malkowski TF, Motala MJ, Ahn BY, Nuzzo RG, Bernhard JT, Lewis JA (2011) Conformal printing of electrically small antennas on three-dimensional surfaces. *Adv Mater* 23(11):1335–1340
3. Ainsley C, Reis N, Derby B (2002) Freeform fabrication by controlled droplet deposition of powder filled melts. *J Mater Sci* 37:3155–3161
4. Alting L, Kimura F, Hansen HN, Bissacco G (2003) Micro engineering. *CIRP Ann Manuf Technol* 52:635–657

5. Ang TH, Sultana FSA, Hutmacher DW, Wong YS, Fuh JYH, Mo XM, Loh HT, Burdet E, Teoh SH (2002) Fabrication of 3D chitosan-hydroxyapatite scaffolds using a robotic dispensing system. *Materials Science & Engineering C-Biomimetic and Supramolecular Systems* 20:35–42
6. Arcaute K, Mann B, Wicker R (2010) Stereolithography of spatially controlled multi-material bioactive poly(ethylene glycol) scaffolds. *Acta Biomaterialia* 6:1047–1054
7. Barry RA, Shepherd RF, Hanson JN, Nuzzo RG, Wiltzius P, Lewis JA (2009) Direct-Write Assembly of 3D Hydrogel Scaffolds for Guided Cell Growth. *Adv Mater* 21:2407–2410
8. Barron, JA, Wu P, Ladouceur HD, Ringeisen BR (2004) Biological laser printing: a novel technique for creating heterogeneous 3-dimensional cell patterns. *Biomed Microdevices* 6:139–147
9. Bartolo PJ (2011) *Stereolithography: materials, processes and applications*. Springer, London
10. Bartolo PJ, Gaspar J (2008) Metal filled resin for stereolithography metal part. *CIRP Ann Manuf Technol* 57:235–238
11. Becker EW, Ehrfeld W, Hagmann P, Maner A, Munchmeyer D (1986) Fabrication of microstructures with high aspect ratios and great structural heights by synchrotron radiation lithography, galvanofarming, and plastic moulding (LIGA process). *Microelec Eng* 4:35–56
12. Beluze L, Bertsch A, Renaud P (1999) Microstereolithography: a new process to build complex 3D objects. In: SPIE symposium on design, test and microfabrication of MEMs/MOEMs, Paris, France
13. Bertsch A, Bernhard P, Vogt C, Renaud P (2000) Rapid prototyping of small size objects. *Rapid Prototyping J* 6:259–266
14. Bertsch A, Heimgartner S, Cousseau P, Renaud P (2001). 3D micromixers—downscaling large-scale industrial static mixers. In: *The 14th IEEE International Conference on Micro Electro Mechanical Systems (MEMS2001)*, Interlaken, Switzerland. pp. 507–510
15. Bertsch A, Heimgartner S, Cousseau P, Renaud P (2001) Static micromixers based on large-scale industrial mixer geometry. *Lab Chip* 1:56–60
16. Bertsch A, Jiguet S, Renaud P (2004) Microfabrication of ceramic components by microstereolithography. *J Micromech Microeng* 14:197–203
17. Bertsch A, Lorenz H, Renaud P (1998). Combining microstereolithography and thick resist UV lithography for 3D microfabrication. In: *Proceedings of the IEEE International Conference on Micro Electro Mechanical Systems (MEMS)*. pp. 18–23.
18. Bertsch A, Lorenz H, Renaud P (1999) 3D microfabrication by combining microstereolithography and thick resist UV lithography. *Sensor Actuator Phys* 73:14–23
19. Bertsch A, Zissi S, Jezequel JY, Corbel S, Andre JC (1997) Microstereophotolithography using a liquid crystal display as dynamic mask generator. *Microsyst Technol* 3:42–47
20. Bertsch A, Jezequel YJ, Andre JC (1997) Study of the spatial resolution of a new 3D micro fabrication process; the microstereolithography using a dynamic mask-generator technique. *J Photochem Photobiol Chem* 107:275–282
21. Bhushan B (2007) *Handbook of nanotechnology*. Springer, New York
22. Billiet T, Vandenhoute M, Schelfhout J, Van Vlierberghe S, Dubruel P (2012) A review of trends and limitations in hydrogel-rapid prototyping for tissue engineering. *Biomaterials* 33:6020–6041
23. Bredt, J.F., Anderson, T.C., Russell, D.B., 2002. Three dimensional printing materials system. US Patent 6,416,850. US Patent and Trademark Office, Z Corporation
24. Brinksmeier E, Riemer O, Stern R (2001). Machining of precision parts and microstructures. In: *Proceedings of the 10th International Conference on Precision Engineering (ICPE)*, Yokohama, Japan, 18–20 July. pp. 3–11
25. Broer DJ, Mol GN, Challa G (1991) In-situ photopolymerization of oriented liquid-crystalline acrylates. *Makromol Chem* 192:59–74
26. Brousseau EB, Dimov SS, Pham DT (2010) Some recent advances in multi-material micro- and nano-manufacturing. *Int J Adv Manuf Technol* 47:161–180
27. Butler EJ, Folk C, Cohen A, Vasilyev NV, Chen R, del Nido PJ, Dupont PE (2011). Metal MEMS tools for beating-heart tissue approximation. In: *2011 IEEE International Conference on Robotics and Automation*, Shanghai, China
28. Buyer's guide, envisionTEC GmbH. Available from www.envisiontec.de
29. Campbell AN, Tanner DM, Soden JM, Stewart DK, Doyle A, Adam E, Gibson M, Abramo M (1997). Electrical and chemical characterization of FIB-deposited insulators. In: *Proceedings of the 23 International Symposium on Testing and Failure Analysis*. pp. 223–230.
30. Cao W, Miyamoto Y (2006) Freeform fabrication of aluminum parts by direct deposition of molten aluminum. *J Mater Process Technol* 173:209–212
31. Cappi B, Özkol E, Ebert J, Telle R (2008) Direct inkjet printing of Si₃N₄: characterization of ink, green bodies and microstructure. *J Eur Ceram Soc* 28:2625–2628
32. Carreño-Morelli E, Martinerie S, Bidaux JE (2007) Three-dimensional printing of shape memory alloys. *Mater Sci Forum* 534–536:477–480
33. Carrozza MC, Croce N, Magnani B, Dario P (1995) A piezoelectric-driven stereolithography-fabricated micropump. *J Micromech Microeng* 5:177–179
34. Cawley JD (1999) Solid freeform fabrication of ceramics. *Curr Opin Solid State Mater Sci* 4:483–489
35. Cesarano J (1999) A review of robocasting technology. In: Dimos D, Danforth SC, Cima MJ (eds) *Solid Freeform and Additive Fabrication*. Materials Research Society, Warrendale
36. Charneau JF, Minev R, Dimov S, Minev E, Su S, Harrysson U (2008). Capability study of the Fcubic direct shell process for casting micro-components. 4M Cross Divisional Report. Cardiff University, Cardiff
37. Chatwin CR, Farsari M, Huang S, Heywood HI, Birch PM, Young RCD, Richardson JD (1998) UV microstereolithography system that uses spatial light modulator technology. *Appl Optic* 37:7514–7522
38. Chen RT, Brown ER, Singh RS (2004). A compact 30 GHz low loss balanced hybrid coupler fabricated using micromachined integrated coax. In: *Proceedings 2004 IEEE Radio and Wireless Conference*, Atlanta, GA
39. Cheng YL, Lin JH, Lai JH, Ke CT, Huang YC (2005). Development of dynamic mask photolithography system. In: *Proceedings of the 2005 IEEE International Conference on Mechatronics*, Taipei, Taiwan. pp. 467–471
40. Choi JW, Ha YM, Won MH, Choi KH, Lee SH (2005). Fabrication of 3-dimensional microstructures using dynamic imageprojection. In: *Proceedings of International Conference on Precision Engineering and Micro/Nano Technology in Asia (ASPEN 2005)*, Shenzhen, China. pp. 472–476
41. Chua CK, Leong KF, Lim CS (2010) *Rapid prototyping: principles and applications*, 3rd edn. World Scientific, Singapore
42. Clare AT, Chalker PR, Davies S, Sutcliffe CJ, Tsoupanos S (2008) Selective laser melting of high aspect ratio 3D nickel–titanium structures two way trained for MEMS applications. *Int J Mech Mater Des* 4:181–187
43. Cohen A, (2004). Going beyond silicon MEMS with EFAB Technology. White paper. Microfabrica Inc., Burbank
44. Cohen A, (2005). EFAB Technology: unlocking the potential of miniaturized medical devices. EVP, Technology and CTO. Microfabrica Inc., Burbank

45. Cohen A, Chen, R (2007). Microfabricated tissue removal instruments for minimally-invasive procedures. In: 19th International Conference of the Society for Medical Innovation and Technology, Sendai, Japan
46. Cohen A, Chen R, Frodis U, Wu MT, Folk C (2010) Microscale metal additive manufacturing of multi-component medical devices. *Rapid Prototyping J* 16:209–215
47. Cohen A, Frodis U, Zhang G, (1998). EFAB: batch production of functional, fully-dense metal parts with micron-scale features. In: Solid Freeform Fabrication Symposium Proceedings, The University of Texas, Austin
48. Cohen A, Kruglick E (2006) EFAB technology and applications. In: Gad-el-Hak M (ed) *The MEMS handbook*, vol 2nd. CRC Press, Boca Raton
49. Cohen A, Wooden S (2005). Monolithic 3-D microfabrication of mechanisms with multiple independently-moving parts. In: Proceedings of IMECE2005: 2005 ASME International Mechanical Engineering Congress and Exposition, Florida.
50. Cohen A, Zhang G, Tseng F, Frodis U, Mansfeld F, Will P (1999). EFAB: rapid, low-cost desktop micromachining of high aspect ratio true 3-D MEMS. In: Proceedings of the IEEE International MEMS 99 Conference. pp. 244–251
51. Crivello JV (1999) The discovery and development of onium salt cationic photoinitiators. *J Polymer Sci Polymer Chem* 37:4241–4254
52. Crocker JE, Harrison S, Sun LLL, Marcus HL (1998) Using SALDVI and SALD with multi-material structures. *J Miner Met Mater Soc* 50:21–23
53. Cumpston BH, Ananthavel SP, Barlow S, Dyer DL, Ehrlich JE, Erskine LL, Heikal AA, Kuebler SM, Lee IYS, McCord-Maughon D, Qin J, Röckel H, Rumi M, Wu XL, Marder SR, Perry JW (1999) Two-photon polymerization initiators for three-dimensional optical data storage and microfabrication. *Nature* 398:51–54
54. Day D, Gu M (1999) Use of two-photon excitation for erasable-writable three-dimensional bit optical data storage in a photo-refractive polymer. *Opt Lett* 24:948–950
55. Debaes C, Vervaeke M, Volckaerts B, Van Erps J, Desmet L, Ottevaere H, Vynck P, Gomez V, Hermanne A, Thienpont H (2005) Low-cost micro-optical modules for board level optical interconnections. *IEEE LEOS Newsletter* 19:12–14
56. Derby B, Reis N (2003) Inkjet printing of highly loaded particulate suspensions. *MRS Bull* 28:815–818
57. Deubel M, Von Freymann G, Wegener M, Pereira S, Busch K, Soukoulis CM (2004) Direct laser writing of three-dimensional photonic-crystal templates for telecommunications. *Nat Mater* 3:444–447
58. Deubel M, Wegener M, Linden S, Von Freymann G, John S (2006) 3D-2D-3D photonic crystal heterostructures fabricated by direct laser writing. *Optic Lett* 31:805–807
59. Dimov, SS, Matthews CW, Glanfield A, Dorrington PA (2006). Roadmapping study in multi-material micro manufacture. In: Proceedings of the Second International Conference on Multi-material Micromanufacture, 4M2006, Grenoble, France, 20–22 September, pp. xi–xxv
60. Doraiswamy A, Jin C, Narayan RJ, Mageswaran P, Mente P, Modi R, Auyeung R, Chrisey DB, Ovsianikov A, Chichkov B (2006) Two photon induced polymerization of organic–inorganic hybrid biomaterials for microstructured medical devices. *Acta Biomaterialia* 2:267–275
61. Dorj B, Park JH, Kim HW (2012) Robocasting chitosan/nano-bioactive glass dual-pore structured scaffolds for bone engineering. *Mater Lett* 73:119–122
62. Dufaud O, Corbel S (2003) Oxygen diffusion in ceramic suspensions for stereolithography. *Chem Eng J* 92:55–62
63. Duoss EB, Twardowski M, Lewis JA (2007) Sol–gel Inks for Direct-Write Assembly of Functional Oxides. *Adv Mater* 19 (21):3485–3489
64. Duty C, Jean D, Lackey WJ (2001) Laser chemical vapor deposition: materials, modeling, and process control. *Int Mater Rev* 46:271–287
65. Ebert J, Özkol E, Zeichner A, Uibel K, Weiss O, Koops U, Telle R, Fischer H (2009) Direct inkjet printing of dental prostheses made of zirconia. *J Dent Res* 88:673–676
66. Ebert R, Regenfuss P, Hartwig L, Klötzer S, Exner H, (2003). Process assembly for μm -scale SLS, reaction sintering, and CVD. In: 4th International Symposium on Laser Precision Microfabrication. Proceedings of SPIE vol. 5063, S.183–188
67. Edinger K (2002) Focused ion beam for direct writing. In: Pique A, Chrisey DB (eds) *Direct write technologies for rapid prototyping applications*. Academic, New York, pp 347–383
68. Edinger K, Melngailis J, Orloff J (1998) Study of precursor gases for focused ion beam insulator deposition. *J Vac Sci Tech B* 16:3311–3314
69. Ehrfeld W, Schmidt A (1998) Recent developments in deep X-ray lithography. *J Vac Sci Technol B* 16:3526–34
70. Evans J, Yang S (2009) Solid freeforming and combinatorial research. *Tsinghua Sci Technol* 14(S1):94–99
71. Exner H, Horn M, Streek A, Hartwig L, Ebert R (2005) First results in laser micro sintering of ceramic materials. *European Congress on Advanced Materials and Processes*, Prague
72. Exner H, Horn M, Streek A, Ullmann F, Hartwig L, Regenfuß P, Ebert R (2008). Laser micro sintering: a new method to generate metal and ceramic parts of high resolution with sub-micrometer powder. In: *Virtual and physical prototyping*, vol 3. Taylor & Francis, New York. pp. 3–11
73. Exner H, Regenfuss P, Hartwig L, Klötzer S, Ebert R (2003). Selective laser micro sintering with a novel process. In: 4th International Symposium on Laser Precision Microfabrication. Proceedings of SPIE, vol. 5063, S.145–151.
74. Farrer RA, LaFratta CN, Li L, Praino J, Naughton MJ, Saleh BEA, Teich MC, Fourkas JT (2006) Selective functionalization of 3-D polymer microstructures. *J Am Chem Soc* 128:1796–1797
75. Fedorovich NE, Oudshroon MH, Geemen D, Hennink WE, Alblas J, Dhert WJA (2009) The effect of photopolymerization on stem cells embedded in hydrogels. *Biomaterials* 30:344–353
76. Formanek F, Takeyasu N, Tanaka T, Chiyoda K, Ishikawa A, Kawata S (2006) Three-dimensional fabrication of metallic nanostructures over large areas by two-photon polymerization. *Opt Express* 14:800–809
77. Foulon F, Stuke M (1993) Argon-ion laser direct-write Al deposition from trialkylamine alane precursors. *Appl Phys A* 56:283–289
78. Freymann GV, Ledermann A, Thiel M, Stauder I, Essig S, Busch K, Wegener M (2010) Three-dimensional nanostructures for photonics. *Adv Funct Mater* 20:1038–1052
79. Galajda P, Ormos P (2001) Complex micromachines produced and driven by light. *Appl Phys Lett* 78:249–251
80. Gaspar J, Bartolo PJ, Duarte FM (2008) Cure and rheological analysis of reinforced resins for stereolithography. *Mater Sci Forum* 587–588:563–567
81. Gebhardt A (2003) *Rapid prototyping*. Hanser Gardner Publications, Inc., Cincinnati (originally published in German)
82. Gibson I, Rosen DW, Stucker B (2010) *Additive manufacturing technologies*. Springer, New York
83. Gotzen R, Reinhardt A (2008) High volume production by RM: challenges and solutions for small parts and MEMS. *International conference on additive technologies*. Ptuj, Slovenia
84. Greulich M, Greul M, Pintat T (1995) Fast, functional prototypes via multiphase jet solidification. *Rapid Prototyping J* 1:20–25
85. Grida I, Evans JRG (2003) Extrusion freeforming of ceramics through fine nozzles. *J Eur Ceram Soc* 23:629–635
86. Guo R, Li Z, Jiang Z, Yuan D, Huang W, Xia A (2005) Log-pile photonic crystal fabricated by two-photon photopolymerization. *J Opt A: Pure Appl Opt* 7:396–699

87. Guo R, Xiao S, Zhai X, Li J, Xia A, Huang W (2006) Micro lens fabrication by means of femtosecond two photon polymerization. *Opt Express* 14:810–816
88. Ha YM, Park IB, Kim HC, Lee SH (2010) Three-dimensional microstructure using partitioned cross-sections in projection microstereolithography. *Int J Precis Eng Manuf* 11:335–340
89. Hadipoespito G, Yang Y, Choi H, Ning G, Li X, (2003). Digital micromirror device based microstereolithography for micro structures of transparent photopolymer and nanocomposites. In: Proceedings of the 14th Solid Freeform Fabrication Symposium, Austin, TX. pp. 13–24
90. Haferkamp H, Ostendorf A, Becker H, Czerner S, Stippler P (2004) Combination of Yb:YAG-disc laser and roll-based powder deposition for the micro-laser sintering. *J Mater Process Tech* 149:623–626
91. Hasegawa T, Nakashima K, Omatsu F, Ikuta K (2008) Multi-directional micro switching valve chip with rotary mechanism. *Sensor Actuator Phys* 143:390–398
92. Hatashi T (2000). Direct 3D forming using TFT LCD mask. In: Proceedings of the 8th International Conference on Rapid Prototyping, Tokyo, Japan. pp. 172–177
93. Heller C, Schwentenwein M, Russmueller G, Varga F, Stampfl J, Liska R (2009) Vinyl esters: low cytotoxicity monomers for the fabrication of biocompatible 3D scaffolds by lithography based additive manufacturing. *J Polymer Sci Polymer Chem* 47:6941–6954
94. Hill RT, Lyon JL, Allen R, Stevenson KJ, Shear JB (2005) Aqueous microfabrication of bioelectronic architectures. *J Am Chem Soc* 127:10707–10711
95. Hoffmann P, Melngailis J, Michler J (2000). Focused ion beam induced deposition of gold and rhodium. In: Proceedings of the Materials Research Society Symposium, vol. 624. pp. 171–175
96. Hon KKB, Li L, Hutchings IM (2008) Direct writing technology—advances and developments. *CIRP Ann Manuf Technol* 57:601–620
97. Huang YM, Jiang CP (2003) Numerical analysis of mask type stereolithography process using dynamic finite element method. *Int J Adv Manuf Technol* 21:649–655
98. Huang YM, Jeng JY, Jiang, CP, Wang JC (2001). Computer supported force analysis and layer imagine for masked rapid prototyping system. In: Proceedings of the 6th International Conference on Computer Supported Cooperative Work in Design, Ontario, Canada. pp. 562–567
99. Hung-Jen Y, Ching-Shiow T, Shan-Hui H, Ching-Lin T (2009) Evaluation of chondrocyte growth in the highly porous scaffolds made by fused deposition manufacturing (FDM) filled with type II collagen. *Biomed Microdevices* 11:615–624
100. Igaki J, Kometani R, Nakamatsu K, Kanda K, Haruyama Y, Ochiai Y (2006) Three-dimensional rotor fabrication by focused-ion-beam chemical-vapor deposition. *Microelectron Eng* 83:1221–1226
101. Ikuta K, Hasegawa T, Adachi T (2001). The optimized SMA micro-pump chip applicable to liquids and gases. In: Thansducers'01 Eurosensors XV Workshop, Munich, Germany
102. Ikuta K, Hasegawa T, Adachi T, Maruo S (2000). Fluid drive chips containing multiple pumps and switching valves for biochemical IC family. In: 13th IEEE International Conference on Microelectro Mechanical Systems (MEMS 2000), Miyazaki, Japan. pp. 739–744
103. Ikuta K, Hirowatari K (1993). Real three-dimensional microfabrication using stereolithography and metal molding. In: Proceedings of the IEEE international Workshop on Microelectromechanical Systems (MEMS '93), Fort Lauderdale. pp. 42–47
104. Ikuta K, Maruo S, Kojoma S (1993). New microstereo lithography for freely movable 3D microstructure. In: Proceedings of the IEEE international Workshop on Microelectromechanical Systems (MEMS '93), Fort Lauderdale. pp. 290–295
105. Ikuta K, Ogata T, Tsubio M, Kojima S, (1996). Development of mass productive microstereolithography. In: Proceedings of the IEEE international Workshop on Microelectromechanical Systems (MEMS), San Diego. pp. 301–305
106. Ikuta K, Sasaki Y, Maegawa H, Maruo S, (2002). Microultrasonic homogenizer chip made by hybrid microstereolithography. In: Symposium on Micrototal Analysis Systems (MicroTAS'02) Conference. Kluwer, Norwell.
107. Jafari MA, Han W, Mohammadi F (2000) A novel system for fused deposition of advanced multiple ceramics. *Rapid Prototyping J* 6:161–175
108. Jayasinghe SN (2007) Bio-electros prays: The development of a promising tool for regenerative and therapeutic medicine. *Biotechnol J* 2:934–937
109. Jiang XS, Qi LH, Luo J, Huang H, Zhou JM (2010) Research on accurate droplet generation for micro-droplet deposition manufacture. *Int J Adv Manuf Technol* 49:535–541
110. Jiguet S, Bertsch A, Renaud P (2002). Microstereolithography and ceramic composite three-dimensional parts. In: Proceedings of the Shaping II conference, Gent, Belgium
111. Johander P, Eberhard W, Necula D, Haasl S, Jung E (2007). Three-dimensional electronics packaging and interconnection 3D PACK. 4M Cross Divisional Report. Cardiff University, Cardiff. pp. 8–22.
112. Johander P, Haasl S, Persson K, Harrysson U (2007). Layer manufacturing as a generic tool for microsystem integration. In: 4M2007 Conference Proceedings, Borovets, Bulgaria.
113. Johander P, Harrysson U, Kaufmann U, Ritzhaupt-Kleissl HJ, (2005). Direct manufacture of ceramic micro components with layered manufacturing methods. In: 4M Conference, Karlsruhe, Germany
114. Kalita SJ, Bose S, Hosick HL, Bandyopadhyay A (2003) Development of controlled porosity polymer-ceramic composite scaffolds via fused deposition modeling. *Materials Science & Engineering C-Biomimetic and Supramolecular Systems* 23:611–620
115. Karam RM, Casler RJ (2003). A new 3D, direct-write, sub-micron microfabrication process that achieves true optical, mechatronic and packaging integration on glass-ceramic substrates. White paper, Invenios, Inc
116. Kawamoto H (2007). Electronic circuit printing, 3D printing and film formation utilizing electrostatic inkjet technology. In: International Conference on Digital Printing Technologies and Digital Fabrication, Anchorage, Alaska. pp. 961–964
117. Kawata S, Sun HB, Tanaka T, Takada K (2001) Finer features for functional microdevices. *Nature* 412:697–698
118. Khalil S, Nam J, Sun W (2005) Multi-nozzle deposition for construction of 3D biopolymer tissue scaffolds. *Rapid Prototyping J* 11:9–17
119. Kim CS, Ahn SH, Jang DY (2012) Review: developments in micro/nanoscale fabrication by focused ion beams. *Vacuum* 86:1014–1035
120. Kim DS, Lee IH, Kwon TH, Cho DW (2004) A barrier embedded Kenics micromixer. *J Micromech Microeng* 14:1294–1301
121. Klein F, Richter B, Striebel T, Franz CM, Freymann GV, Wegener M, Bastmeyer M (2011) Two-component polymer scaffolds for controlled three-dimensional cell culture. *Adv Mater* 23:1341–1345
122. Klein S, Barsella A, Leblond H, Bulou H, Fort A, Andraud C, Lemercier G, Mulatier JC, Dorkenoo K (2005) One-step waveguide and optical circuit writing in photopolymerizable materials processed by two-photon absorption. *Appl Phys Lett* 86:211118 (1)–211118(3)
123. Klosterman DA, Chartoff RP, Osborne NR, Graves GA, Lightman A, Han GW, Bezeredi A, Rodrigues S, Pak S, Kalmanovich G, Dodin L, Tu S (1998) Direct fabrication of ceramics, CMCs by rapid prototyping. *Am Ceram Soc Bull* 77:69–74

124. Ko SH, Chung J, Hotz N, Nam KH, Grigoropoulos CP (2010) Metal nanoparticle direct inkjet printing for low-temperature 3D micro metal structure fabrication. *J Micromech Microeng* 20:125010 (7 pp)
125. Ko SH, Pan H, Grigoropoulos CP, Luscombe CK, Fréchet J, Poulidakos D (2007) All-inkjet-printed flexible electronics fabrication on a polymer substrate by low-temperature high-resolution selective laser sintering of metal nanoparticles. *Nanotechnology* 18:345202
126. Kobayashi K, Ikuta K (2005). Development of free surface microstereolithography with ultra high resolution to fabricate hybrid 3-D microdevices. In: *IEEE International Symposium on Micro-nano Mechatronics and Human Science*
127. Kometani R, Funabiki R, Hoshino T, Kanda K, Haruyama Y, Kaito T (2006) Cell wall cutting tool and nano-net fabrication by FIB-CVD for subcellular operations and analysis. *Microelectron Eng* 83:1642–1645
128. Kometani R, Hoshino T, Kondo K, Kanda K, Haruyama Y, Kaito J (2005) Performance of nanomanipulator fabricated on glass capillary by focused ion-beam chemical vapor deposition. *J Vac Sci Technol B* 23:298–301
129. Kometani R, Morita T, Watanabe K, Hoshino T, Kondo K, Kanda K (2004) Nanomanipulator and actuator fabrication on glass capillary by focused-ion beam-chemical vapor deposition. *J Vac Sci Technol B* 22:257–263
130. Lai WH, Chen CC (2005) Effect of oxidation on the breakup and monosized droplet generation of the molten metal jet. *AtomizSpr* 15:81–102
131. Lam CXF, Mo XM, Teoh SH, Hutmacher DW (2002) Scaffold development using 3D printing with a starch-based polymer. *Mater Sci Eng C* 20:49–56
132. Lan PX, Lee JW, Seol YJ, Cho DW (2009) Development of 3D PPF/DEF scaffolds using micro-stereolithography and surface modification. *J Mater Sci Mater Med* 20:271–279
133. Landers R, Hübner U, Schmelzeisen R, Mülhaupt R (2002) Rapid prototyping of scaffolds derived from thermoreversible hydrogels and tailored for applications in tissue engineering. *Biomaterials* 23:4437–4447
134. Landers R, Mülhaupt R (2000) Desktop manufacturing of complex objects, prototypes and biomedical scaffolds by means of computer-assisted design combined with computer-guided 3D plotting of polymers and reactive oligomers. *Macromol Mater Eng* 282:17–21
135. Lanzetta M, Sachs E (2003) Improved surface finish in 3D printing using bimodal powder distribution. *Rapid Prototyping J* 9:157–166
136. Lass N, Tropmann A, Ernst A, Zengerle R, Koltay P (2011). Rapid prototyping of 3d microstructures by direct printing of liquid metal at temperatures up to 500°C using the starjet technology. In: *16th Solid-State Sensors, Actuators and Microsystems International Conference (TRANSDUCERS)*, Beijing, China. pp. 1452–1455
137. Ledermann A, Wegener M, Von Freymann G (2010) Rhombicuboctahedral three-dimensional photonic quasicrystals. *Adv Mater* 22:2363–2366
138. Lee JW, Lan PX, Kim B, Lim G, Cho DW (2008) Fabrication and characteristic analysis of a poly(propylene fumarate) scaffold using micro-stereolithography technology. *J Biomed Mater Res B Appl Biomater* 87:1–9
139. Lee JW, Lee IH, Cho DW (2006) Development of micro-stereolithography technology using metal powder. *Microelect Eng* 83:1253–1256
140. Lee KJ, Jun BH, Kim TH, Joung J (2006) Direct synthesis and inkjetting of silver nanocrystals toward printed electronics. *Nanotechnology* 17:2424–2428
141. Lee Y, Lu X, Hao Y, Yang SF, Ubic R, Evans JRG, Parini CG (2007) Rapid prototyping of ceramic millimeterwave metamaterials: Simulations and experiments. *Microw Opt Technol Lett* 49(9):2090–2093
142. Lee Y, Lu X, Hao Y, Yang SF, Ubic R, Evans JRG, Parini CG (2007) Directive millimetre-wave antenna based on freeformed woodpile EBG structure. *Electron Lett* 43(4):195–196
143. Lee Y, Lu X, Hao Y, Yang SF, Evans JRG, Parini CG (2008) Directive millimetrewave antennas using freeformed ceramic metamaterials in planar and cylindrical forms. In: *IEEE antennas and propagation society international symposium*, vol. 1–9, San Diego, CA, 5–11 Jul 2008. pp. 2242–2245
144. Lee KS, Kim RH, Yang DY, Park SH (2008) Advances in 3D nano/microfabrication using two-photon initiated polymerization. *Prog Polym Sci* 33:631–681
145. Lee Y, Lu X, Hao Y, Yang SF, Evans JRG, Parini CG (2009) Low-profile directive millimeter-wave antennas using free-formed three-dimensional (3-D) electromagnetic bandgap structures. *IEEE Trans Antenn Propag* 57(10):2893–2903
146. Lee Y, Lu X, Hao Y, Yang SF, Evans JRG, Parini CG (2010) Narrow-beam azimuthally omni-directional millimetre-wave antenna using freeformed cylindrical woodpile cavity. *IEE Proc Microwaves Antenn Propag* 4(10):1491–1499
147. Lehmann O, Stuke M (1994) Three-dimensional laser direct writing of electrically conducting and isolating microstructures. *Mater Lett* 21:131–135
148. Lehua Q, Xiaoshan J, Jun L, Xianghui H, Hejun L (2010) Dominant factors of metal jet breakup in micro droplet deposition manufacturing technique. *Chin J Aeronaut* 23:495–500
149. Lejeune M, Chartier T, Dossou-Yovo C, Noguera R (2009) Ink-jet printing of ceramic micro-pillar arrays. *J Eur Ceram Soc* 29:905–911
150. Li R, Ashgriz N, Chandra S (2008) Droplet generation from pulsed micro jets. *Exp Therm Fluid Sci* 32:1679–1686
151. Lim TW, Son Y, Yang DY, Kong HJ, Lee KS (2010) Selective ablation-assisted two-photon stereolithography for effective nano- and microfabrication. *Appl Phys A* 103:1111–1116
152. Liu Q, Orme M (2001) High precision solder droplet printing technology and the state-of-the art. *J Mater Process Technol* 115:271–283
153. Liu Q, Orme M (2001) On precision droplet-based net-form manufacturing technology. *Proc IME B J Eng Manufac* 215:1333–1355
154. Liu VA, Bhatia SN (2002) Three-dimensional patterning of hydrogels containing living cells. *Biomed Microdevices* 4:257–266
155. Longo DM, Hull R (2000). Direct focused ion beam writing of printheads for pattern transfer utilizing microcontact printing. In: *Proceedings of the Materials Research Society Symposium*, vol. 624. pp. 157–160
156. Lorenz AM, Sachs EM, Allen SM (2004). Techniques for infiltration of a powder metal skeleton by a similar alloy with melting point depressed. U.S. Patent 6,719,948. US Patent and Trademark Office, Massachusetts Institute of Technology.
157. Lu K, Reynolds WT (2008) 3DP process for fine mesh structure printing. *Powder Technol* 187:11–18
158. Lu S, Anseth KS (1999) Photopolymerization of multilaminated poly(HEMA) hydrogels for controlled release. *J Contr Release* 57:291–300
159. Lu X, Yang S, Evans JRG (2007) Dose uniformity of fine powders in ultrasonic microfeeding. *Powder Technol* 175:63–72
160. Lu X, Lee Y, Yang SF, Hao Y, Ubic R, Evans JRG, Parini CG (2008) Fabrication of electromagnetic crystals by extrusion free-forming. *Metamaterials* 2(1):36–44
161. Lu X, Lee Y, Yang SF, Hao Y, Ubic R, Evans JRG, Parini CG (2009) Fabrication of millimeter-wave electromagnetic bandgap crystals using microwave dielectric powders. *J Am Ceram Soc* 92(2):371–378
162. Lu X, Lee Y, Yang SF, Hao Y, Evans JRG, Parini CG (2009) Fine lattice structures fabricated by extrusion freeforming: process variables. *J Mater Process Tech* 209(10):4654–4661

163. Lu X, Lee Y, Yang SF, Hao Y, Evans JRG, Parini CG (2009) Extrusion freeforming of millimeter wave electromagnetic bandgap (EBG) structures. *Rapid Prototyping Journal* 15(1):42–51
164. Lu X, Lee Y, Yang SF, Hao Y, Evans JRG, Parini CG (2010) Solvent-based paste extrusion solid freeforming. *J Eur Ceram Soc* 30(1):1–10
165. Lu XS, Chen LF, Amini N, Yang SF, Evans JRG, Guo ZX (2012) Novel methods to fabricate macroporous 3D carbon scaffolds and ordered surface mesopores on carbon filaments. *J Porous Mat* 19(5):529–536
166. Madden JD, Hunter IW (1996) Three-dimensional microfabrication by localized electrochemical deposition. *J Microelectromech Syst* 5:24–32
167. Madou MJ (2002) *Fundamentals of microfabrication: the science of miniaturization*, 2nd edn. CRC Press, New York
168. Mariani M, Rosatini F, Vozzi G, Previti A, Ahluwalia A (2006) Characterization of tissue-engineered scaffolds microfabricated with PAM. *Tissue Eng* 12:547–557
169. Maruo S, Ikuta K, Korogi H (2003) Submicron manipulation tools driven by light in a liquid. *Appl Phys Lett* 82:133–135
170. Maruo S, Kawata S (1998) Two-photon-absorbed near-infrared photopolymerization for three-dimensional microfabrication. *IEEE ASME J Microelectromech Syst* 7:411–415
171. Masuzawa T (2000) State of the art of micro-machining. *CIRP Ann Manuf Technol* 49:473–488
172. Matsui S (2007) Focused-ion-beam deposition for 3-D nanostructure fabrication. *Nucl Instrum Meth B* 257:758–764
173. Melchels FPW, Feijen J, Grijpma DW (2010) A review on stereolithography and its applications in biomedical engineering. *Biomaterials* 31:6121–6130
174. Melchels FPW, Domingos MAN, Klein TJ, Malda J, Bartolo PJ, Huttmacher DW (2012) Additive manufacturing of tissues and organs. *Progr Polymer Sci* 37:1079–1104
175. Michna S, Wu W, Lewis JA (2005) Concentrated hydroxyapatite inks for direct-write assembly of 3-D periodic scaffolds. *Biomaterials* 26:5632–5639
176. MicroFab Inc. (2012). Available from www.MicroFab.com
177. microTEC (2012). Products and applications, microTEC Gesellschaft für Mikrotechnologie mbH. Available from www.microtec-d.com
178. Mihailov S, Lazare S (1993) Fabrication of refractive microlens arrays by excimer laser ablation of amorphous teflon. *Appl Optic* 32:6211–6218
179. Miranda P, Pajares A, Saiz E, Tomsia AP, Guiberteau F (2008) Mechanical properties of calcium phosphate scaffolds fabricated by robocasting. *J Biomed Mater Res A* 85A:218–227
180. Mironov V, Prestwich G, Forgacs G (2007) Bioprinting living structures. *J Mater Chem* 17:2054–2060
181. Mizeikis V, Juodkakis S, Tarozaitis R, Juodkazyte J, Juodkakis K, Misawa H (2007) Fabrication and properties of metallo-dielectric photonic crystal structures for infrared spectral region. *Opt Express* 15:8454–8464
182. Monneret S, Loubere V, Corbel S (1999) Microstereolithography using dynamic mask generator and a non-coherent visible light source. *Proc SPIE* 3680:553–561
183. Monneret S, Provin C, Gall HL, Corbel S (2002) Microfabrication of freedom and articulated alumina-based components. *Microsyst Technol* 8:368–374
184. Morgan JC (1998) Focused ion beam mask repair. *Solid State Tech* 41:61–67
185. Nagel DJ (2002) Technologies for micrometer and nanometer pattern and material transfer. In: Pique A, Chrisey DB (eds) *Direct write technologies for rapid prototyping applications*. Academic, New York, pp 557–701
186. Nakamoto T, Yamaguchi K, (1996). Consideration on the producing of high aspect ratio micro parts using UV sensitive photopolymer. In: *Proceedings of 7th International Symposium on Micro Machine and Human Science*, pp. 53–58.
187. Narahara H, Tanaka F, Kishinami T, Igarashi S, Saito K (1999) Reaction heat effects on initial linear shrinkage and deformation in stereolithography. *Rapid Prototyping J* 5:120–128
188. Neumann J, Wiekling KS, Kip D (1999) Direct laser writing of surface reliefs in dry self-developing photopolymer films. *Appl Opt* 38:5418–5423
189. Noguera R, Lejeune M, Chartier T (2005) 3D fine scale ceramic components formed by ink-jet prototyping process. *J Eur Ceram Soc* 25:2055–2059
190. Park IB, Ha YM, Lee SH (2010) Cross-section segmentation for improving the shape accuracy of microstructure array in projection microstereolithography. *Int J Adv Manuf Technol* 46:151–161
191. Park SH, Lim TW, Yang DY, Kim RH, Lee KS (2006) Fabrication of a bunch of sub-30-nm nanofibers inside microchannels using photopolymerization via a long exposure technique. *Appl Phys Lett* 89:173131–173133
192. Parker ST, Domachuk P, Amsden J, Bressner J, Lewis JA, Kaplan DL, Omenetto FG (2009) Biocompatible Silk Printed Optical Waveguides. *Adv Mater* 21:2411–2415
193. Petsch T, Regenfuss P, Ebert R, Hartwig L, Klötzer S, Brabant TH, Exner H (2004). Industrial laser micro sintering. In: *Proceedings of the 23rd International Congress on Applications of Lasers and Electro-Optics*, Erlangen, Germany. pp. 413–424
194. Priest JW, Smith C, DuBois P (1997). Liquid metal jetting for printing metal parts. In: *Solid Freeform Fabrication Symposium*, Texas, USA
195. Provin C, Monneret S (2002) Complex ceramic-polymer composite microparts made by microstereolithography. *IEEE Trans Electron Packag Manuf* 25:59–63
196. Provin C, Monneret S, Gall HL, Corbel S (2003) Three-dimensional ceramic microcomponents made using microstereolithography. *Adv Mater* 15:994–997
197. Qin Y (2010) *Micro-manufacturing engineering and technology*. Elsevier, Oxford
198. Qin Y, Brockett A, Ma Y, Razali A, Zhao J, Harrison C, Pan W, Dai X, Loziak D (2010) Micro manufacturing: research, technology outcomes and development issues. *Int J Adv Manuf Technol* 47:821–837
199. Quinn DJ, Spearing SM, Ashby MF, Fleck NA (2006) A systematic approach to process selection in MEMS. *J Microelectromech Syst* 15:1039–1050
200. Regenfuss P, Ebert R, Exner H (2007) Laser micro sintering: a versatile instrument for the generation of microparts. *Laser Technik Journal* 4:26–31
201. Regenfuss P, Hartwig L, Klötzer S, Ebert R, Brabant TH, Petsch T, Exner H (2005) Industrial freeform generation of micro tools by laser micro sintering. *Rapid Prototyping J* 11:18–25
202. Regenfuss P, Hartwig L, Klötzer S, Ebert R, Exner H (2003). Microparts by a novel modification of selective laser sintering. In: *Rapid Prototyping and Manufacturing Conference*, Chicago, USA
203. Regenfuss P, Streek A, Hartwig L, Klötzer S, Brabant TH, Horn M, Ebert R, Exner H (2007) Principles of laser micro sintering. *Rapid Prototyping J* 13:204–212
204. Reinhardt C, Passinger S, Chichkov B, Marquart C, Radko I, Bozhevolnyi S (2006) Laser-fabricated dielectric optical components for surface plasmon polaritons. *Opt Lett* 31:1307–1309
205. Reyntjens S, Puers R (2001) A review of focused ion beam applications in microsystem technology. *J Micromech Microeng* 11:287–300
206. Sachs EM, Cima M.J, Caradonna MA, (2003). Jetting layers of powder and the formation of fine powder beds thereby. US Patent

- 6,596,224. US Patent and Trademark Office, Massachusetts Institute of Technology
207. Sachs EM, Haggerty JS, Cima MJ, (1993). Three-dimensional printing techniques. US Patent 5,204,055. US Patent and Trademark Office, Massachusetts Institute of Technology
 208. Scheffer P, Bertsch A, Corbel S, Jejequel JY, Andre JC (1997) Industrial photochemistry XXIV. Relations between light flux and polymerized depth in laser stereolithography. *J Photochem Photobiol Chem* 107:283–290
 209. Schlie S, Ngezahayo A, Ovsianikov A, Fabian T, Kolb HA, Haferkamp H, Chichkov BN (2007) Three-dimensional cell growth on structures fabricated from ORMOCER by two-photon polymerization technique. *J Biomater Appl* 22:275–287
 210. Schiele NR, Koppes RA, Corr DT, Ellison KS, Thompson DM, Ligon LA, Lippert TKM, Chrisey DB (2009) Laser direct writing of combinatorial libraries of idealized cellular constructs: Biomedical applications. *Appl Surf Sci* 255:5444–5447
 211. Schuck H, Bauerfeld F, Sauer D, Harzic RL, Velten T, Riemann I, König K, (2007). Rapid prototyping of 3D micro- nanostructures to explore cell behavior. In: 4M Conference Proceedings, Ingbert, Germany. pp. 16–23
 212. Schuurman W, Khristov V, Pot MW, van Weeren PR, Dhert WJA, Malda J (2011) Bioprinting of hybrid tissue constructs with tailorable mechanical properties. *Biofabrication* 3:021001
 213. Schuster M, Turecek C, Weigel G, Saf R, Stampfl J, Varga F, Liska R (2009) Gelatin-based photopolymers for bone replacement materials. *J Polymer Sci Polymer Chem* 47:7078–7089
 214. Seet KK, Mizeikis V, Matsuo S, Juodkazis S, Misawa H (2005) Three-dimensional spiral—architecture photonic crystals obtained by direct laser writing. *Adv Mater* 17:541–545
 215. Seitz H, Rieder W, Leukers B, Tille C (2005) Three dimensional printing of porous ceramic scaffolds for bone tissue engineering. *J Biomed Mater Res* 74B:782–788
 216. Serbin J, Chichkov BN, Houbertz R (2003) Three-dimensional nanostructuring of hybrid materials by two-photon polymerization. *Proc SPIE* 5222:171–177
 217. Shepherd JNH, Parker ST, Shepherd RF, Gillette MU, Lewis JA, Nuzzo RG (2011) 3D Microperiodic Hydrogel Scaffolds for Robust Neuronal Cultures. *Adv Funct Mater* 21:47–54
 218. Shoji S, Smith N, Kawata S (1999) Photofabrication of a photonic crystal using interference of a UV laser. *Proc SPIE* 3740:541–544
 219. Shoji S, Sun HB, Kawata S (2003) Photofabrication of wood-pile three-dimensional photonic crystals using four-beam interference. *Appl Phys Lett* 83:608–610
 220. Simon JL, Michna S, Lewis JA, Rekow ED, Thompson VP, Smay JE, Yampolsky A, Parsons JR, Ricci JL (2007) In vivo bone response to 3D periodic hydroxyapatite scaffolds assembled by direct ink writing. *J Biomed Mater Res A* 83A:747–758
 221. Smay JE, Gratson GM, Shepherd RF, Cesarano J, Lewis JA (2002) Directed colloidal assembly of 3D periodic structures. *Adv Mater* 14:1279–1283
 222. Stampfl J, Fouad H, Seidler S, Liska R, Schwager F, Woesz A, Fratzl P (2004) Fabrication and moulding of cellular materials by rapid prototyping. *Int J Mater Prod Tech* 21:285–96
 223. Staude I, Von Freymann G, Essig S, Busch K, Wegener M (2011) Waveguides in three-dimensional photonic-bandgap materials by direct laser writing and silicon double inversion. *Optic Lett* 36:67–69
 224. Straub M, Nguyen LH, Fazlic A, Gu M (2004) Complex-shaped three-dimensional microstructures and photonic crystals generated in a polysiloxane polymer by two-photon micro-stereolithography. *Opt Mater* 27:359–364
 225. Straub M, Ventura M, Gu M (2003) Multiple higher-order stop gaps in infrared polymer photonic crystals. *Phys Rev Lett* 91:043901
 226. Streek A, Regenfus P, Ullmann F, Hartwig L, Ebert R, Exner Hm (2006). Processing of silicon carbide by laser micro sintering. In: The Proceedings of the 17th Annual SFF Symposium. pp. 349–385.
 227. Stuke M, Mueller K, Mueller T, Hagedorn R, Jaeger M, Fuhr G (2005) Laser- direct-write creation of three-dimensional orest microcages for contact-free trapping, handling and transfer of small polarizable neutral objects in solution. *Appl Physic A* 81:915–922
 228. Subramanian K, Vail N, Barlow J, Marcus H (1995) Selective laser sintering of alumina with polymer binders. *Rapid Prototyping J* 1:24–35
 229. Subramanian V, Fréchet JMJ, Chang PC, Huang DC, Lee JB, Molesa SE, Murphy AR, Redinger DR, Volkman SK (2005) Progress toward development of all-printed RFID tags: materials, processes, and devices. *Proc IEEE* 93:1330–1338
 230. Sun C, Fang N, Wu DM, Zhang X (2005) Projection micro-stereolithography using digital micro-mirror dynamic mask. *Sensor Actuator Phys I* 21:113–120
 231. Sun H, Kawakami T, Xu Y, Ye J, Matuso S, Misawa H, Miwa M, Kaneko R (2000) Real three-dimensional microstructures fabricated by photopolymerization of resins through two-photon absorption. *Opt Lett* 25:1110–1112
 232. Sun HB, Matsuo S, Misawa H (1999) Three-dimensional photonic crystal structures achieved with two-photon absorption photopolymerization of resin. *Appl Phys Lett* 74:786–788
 233. Sun L, Parker ST, Syoji D, Wang X, Lewis JA, Kaplan DL (2012) Direct-write assembly of 3D silk/hydroxyapatite scaffolds for bone co-cultures. *Advanced Healthcare Materials* 1:729–735
 234. Suzumori K, Koga A, Haneda R (1994) Micro fabrication of integrated FMAs using stereolithography. *IEEE MEMS* 114:136–141
 235. Takagi T, Nakajima N (1993). Photoforming applied to fine machining. In: Proceedings of 4th International Symposium on Micro Machine and Human Science (MHS '93). pp. 173–178.
 236. Takagi, T., Nakajima, N., 1994. Architecture combination by micro photoforming process. In: 7th IEEE Workshop on Micro Electro Mechanical Systems (MEMS '94), Oiso, Japan. pp. 211–216
 237. Tay B, Edirisinghe MJ (2001) Investigation of some phenomena occurring during continuous ink-jet printing of ceramics. *J Mater Res* 16:373–384
 238. Thian SCH, Tang Y, Fuh JYH, Wong YS, Lu L, Loh HT (2006) Micro-rapid-prototyping via multi-layered photo-lithography. *Int J Adv Manuf Technol* 29:1026–1032
 239. Thiel M, Rill MS, Freymann GV, Wegener M (2009) Three-dimensional bi-chiral photonic crystals. *Adv Mater* 21:4680–4682
 240. Thienpont H, Baukens V, Ottevaere H, Volckaerts B, Tuteleers P, Vynck P, Vervaeke M, Debaes C, Verschaffelt G, Hermanne A, Veretennicoff I (2001) Free-space micro-optical modules: the missing link for photonic interconnects to silicon chips. *Opto-Electronics Review* 9:238–247
 241. Tirella A, Vozzi G, Ahluwalia A (2008) Biomimicry of PAM Microfabricated Hydrogel Scaffold. Springfield, Soc Imaging Science & Technology
 242. Tirella A, Orsini A, Vozzi G, Ahluwalia A (2009) A phase diagram for microfabrication of geometrically controlled hydrogel scaffolds. *Biofabrication*, 1
 243. Tirella A, De Maria C, Criscenti G, Vozzi G, Ahluwalia A (2012) The PAM(2) system: a multilevel approach for fabrication of complex three-dimensional microstructures. *Rapid Prototyping J* 18:299–307
 244. Tropmann A, Lass N, Paust N, Metz T, Ziegler C, Zengerle R, Koltay P (2011) Pneumatic dispensing of nano- to picoliter droplets of liquid metal with the StarJet method for rapid prototyping of metal microstructures. *Microfluid Nanofluid* 12:75–84
 245. Tse AL, Hesketh PJ, Rosen DW (2001). Stereolithography on silicon for microfluidics and microsensor packaging. In: 4th

- International Workshop on High Aspect Ratio Micro Structure Technology (HARMST '01), Baden-Baden, Germany
246. Tse AL, Hesketh PJ, Rosen DW, Gole JL (2003) Stereolithography on silicon for microfluidics and microsensor packaging. *Microsyst Technol* 9:319–323
 247. Ullett JS, Benson-Tolle T, Schultz JW, Chartoff RP (1999) Thermal-expansion and fracture toughness properties of parts made from liquid crystal stereolithography resins. *Mater Des* 20:91–97
 248. Ullett JS, Schultz JW, Chartoff RP (2000) Novel liquid crystal resins for stereolithography. *Rapid Prototyping J* 6:8–17
 249. Varadan VK, Jiang S, Varadan VV (2001) *Microstereolithography and other fabrication techniques for 3D MEMS*. Wiley, New York
 250. Vorndran E, Klammert U, Klarner M, Grover LM, Barralet JE, Gbureck U (2009) 3D printing of β -tricalcium phosphate ceramics. *Dent Mater* 25:e18–e19
 251. Vozzi G, Ahluwalia A (2007) Microfabrication for tissue engineering: rethinking the cells-on-a scaffold approach. *J Mater Chem* 17:1248–1254
 252. Vozzi G, Flaim CJ, Bianchi F, Ahluwalia A, Bhatia S (2002) Microfabricated PLGA scaffolds: a comparative study for application to tissue engineering. *Materials Science & Engineering C-Biomimetic and Supramolecular Systems* 20:43–47
 253. Vozzi G, Previti A, Ciaravella G, Ahluwalia A (2004) Microfabricated fractal branching networks. *J Biomed Mater Res A* 71A:326–333
 254. Walters P, Ieropoulos I, McGoran D (2011). Digital fabrication of a novel bio-actuator for bio-robotic art and design. In: *International Conference on Digital Printing Technologies and Digital Fabrication 2011*, Minneapolis, MN. pp. 496–499
 255. Wang F, Shor L, Darling A, Khalil S, Güceri S, Lau A (2004) Precision extruding deposition and characterization of cellular poly-epsilon-caprolactone tissue scaffolds. *Rapid Prototyping J* 10:42–49
 256. Wanke MC, Lehmann O, Muller K, Wen Q, Stuke M (1997) Laser rapid prototyping of photonic band-gap microstructures. *Science* 275:1284–1286
 257. William K, Maxwell J, Larsson K, Boman M (1999). Freeform fabrication of functional microsolenoids, electromagnets and helical springs using high pressure laser chemical vapour deposition. In: *Proceedings of the 12th IEEE International Conference on Micro Electro Mechanical Systems (MEMS '99)*. pp. 232–237.
 258. Woodfield TBF, Malda J, de Wijn J, Péters F, Riesle J, Van Blitterswijk CA (2004) Design of porous scaffolds for cartilage tissue engineering using a three-dimensional fiber-deposition technique. *Biomaterials* 25:4149–4161
 259. Xia Y, Whitesides GM (1998) Soft lithography. *Angew Chem Int Ed* 37:550–75
 260. Xiong Z, Yan YN, Zhang RJ, Sun L (2001) Fabrication of porous poly(L-lactic acid) scaffolds for bone tissue engineering via precise extrusion. *Scr Mater* 45:773–779
 261. Xu G, Zhao W, Tang Y, Lu B (2006) Novel stereolithography system for small size objects. *Rapid Prototyping J* 12:12–17
 262. Yamaguchi K (2003) Generation of 3-dimensional microstructure by metal jet. *Microsystem Technol* 9:215–219
 263. Yamaguchi K, Sakai K, Yamanka T, Hirayama T (2000) Generation of three-dimensional micro structure using metal jet. *Precision Eng* 24:2–8
 264. Yang S, Evans JRG (2004) A dry powder jet printer for dispensing and combinatorial research. *Powder Technol* 142:219–222
 265. Yang S, Evans JRG (2007) Metering and dispensing of powder; the quest for new solid freeforming techniques. *Powder Technol* 178:56–72
 266. Yang HY, Yang SF, Chi XP, Evans JRG (2006) Fine ceramic lattices prepared by extrusion freeforming. *J Biomed Mater Res B Appl Biomater* 79B(1):116–121
 267. Yang HY, Yang SF, Chi XP, Evans JRG, Thompson I, Cook RJ, Robinson P (2008) Sintering behaviour of calcium phosphate filaments for use as hard tissue scaffolds. *J Eur Ceram Soc* 28(1):159–167
 268. Yang HY, Thompson I, Yang SF, Chi XP, Evans JRG, Cook RJ, Robinson P (2008) Dissolution characteristics of extrusion freeformed hydroxyapatite-tricalcium phosphate scaffolds. *J Mater Sci Mater Med* 19(11):3345–3353
 269. Yang SF, Yang HY, Chi XP, Evans JRG, Thompson I, Cook RJ, Robinson P (2008c) Rapid prototyping of ceramic lattices for hard tissue scaffolds. *Mater Des* 29:1802–1809
 270. Yang HY, Yang SF, Chi XP, Evans JRG (2010) Mechanical strength of extrusion freeformed calcium phosphate filaments. *J Mater Sci Mater Med* 21(5):1503–1510
 271. Yim P (1996). The role surface oxidation in the break-up of laminar liquid metal jets. Ph.D. thesis, MIT, Cambridge, MA
 272. Young RJ, Poretz J (1995) Focused ion beam insulator deposition. *J Vac Sci Tech B* 13:2576
 273. Yu T, Ober CK, Kuebler SM, Zhou W, Marder SR, Perry JW (2003) Chemically amplified positive resists for two photon three-dimensional microfabrication. *Adv Mater* 15:517–521
 274. Zein I, Hutmacher DW, Tan KC, Teoh SH (2002) Fused deposition modeling of novel scaffold architectures for tissue engineering applications. *Biomaterials* 23:1169–1185
 275. Zhang X, Jiang XN, Sun C (1998) Micro-stereolithography for MEMS. *Micro electro mechanical systems (MEMS)*. *ASME* 66:3–9
 276. Zhang X, Jiang X, Sun C (1999) Micro-stereolithography of polymeric and ceramic microstructures. *Sensor Actuator Phys* 77:149–156
 277. Zhang YL, Chen QD, Xia H, Sun HB (2010) Designable 3D nanofabrication by femtosecond laser direct writing. *Nano Today* 5:435–448
 278. Zhou C, Chen Y (2012) Additive manufacturing based on optimized mask video projection for improved accuracy and resolution. *J Manuf Process* 14:107–118
 279. Zhuo X, Yongnian Y, Shenguo W, Renji Z, Chao Z (2002) Fabrication of porous scaffolds for bone tissue engineering via low-temperature deposition. *Scr Mater* 46:771–776776
 280. Zissi S, Bertsch A, Jejequel JY, Corbel S, Lougnot DJ, Andre JC (1996) Stereolithography and microtechniques. *Microsyst Technol* 2:97–102